Plasma sputtering synthesis of nanocatalyst for fuel cells: Experiments and molecular dynamics simulations

Pascal Brault

GREMI, UMR7344 CNRS Université d'Orléans,
Orléans, France

pascal.brault@univ-orleans.fr

http://www.univ-orleans.fr/gremi/pascal-brault

Outline

- About fuel cell catalysts and electrodes
- Plasma sputtering insights
- DC magnetron sputtering of catalyst for fuel cells
- HiPIMS deposition
- Magnetron gas aggregation nanocluster source
- Molecular dynamics simulation of plasma sputtering catalysts growth
- Perspectives

About fuel cell catalysts and electrodes

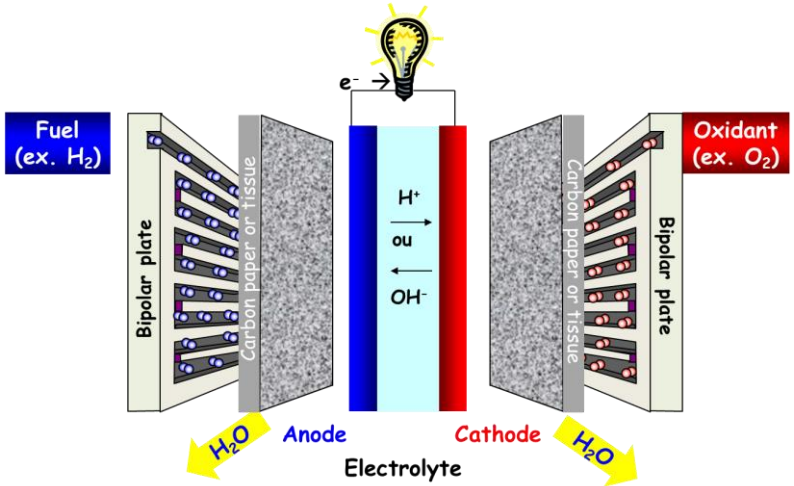

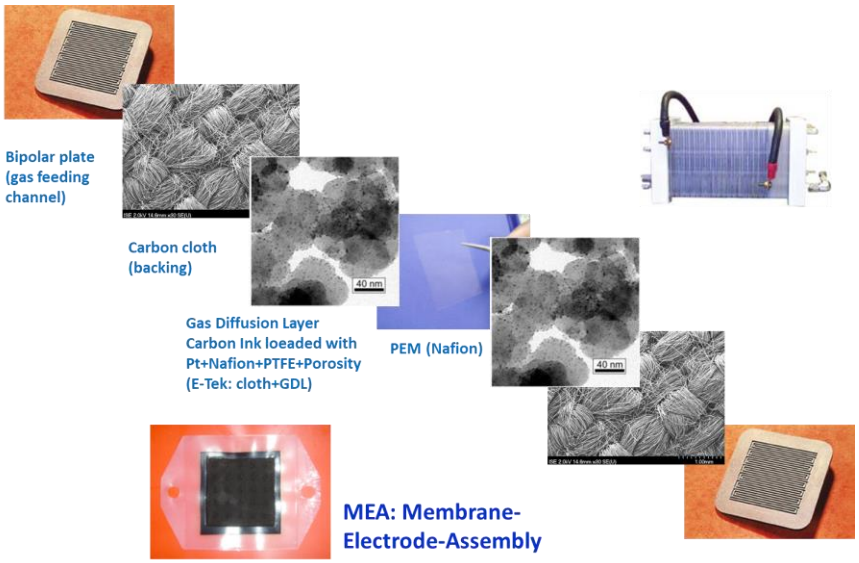

- Proton exchange Membrane Fuel Cell
- Electrochemical DC current generator
- GES free **$H_2 + 1/2\ O_2 \rightarrow H_2O$ + electrical current + heat (90% efficiency!!)**
- Issues:
  - Reducing noble metal catalysts content
  - Increasing performances

About fuel cell catalysts and electrodes

PEMFC: Active phase

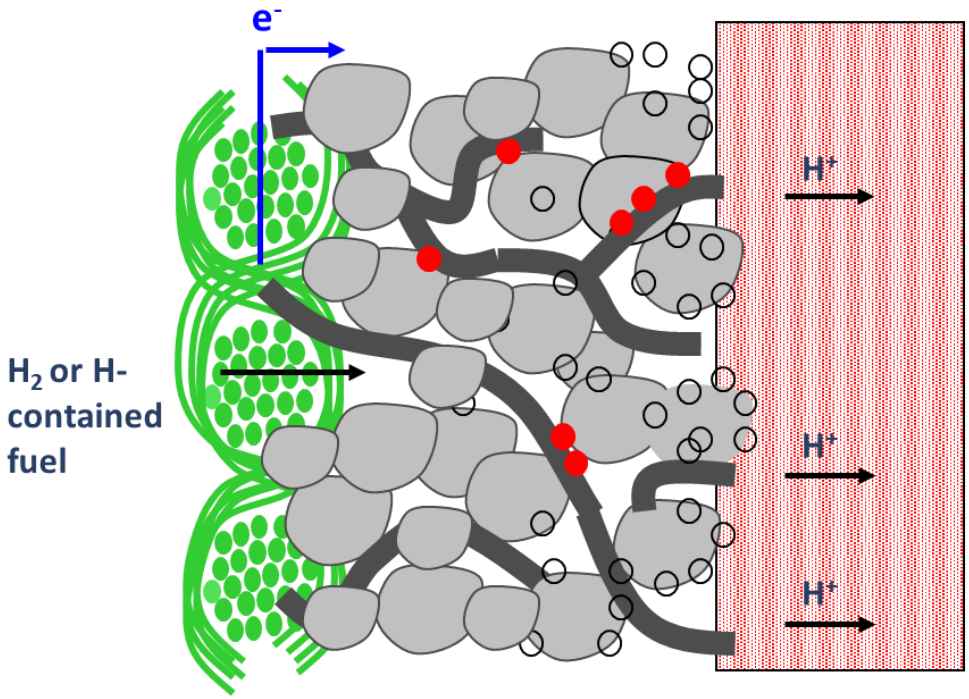

Catalyst is Pt or Pt alloy or …

Cathode

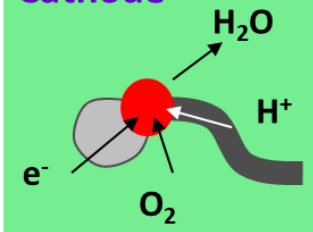

Catalyst +Electrolyte
+ Conducting material
are required simultaneously
for the reactions

Anode

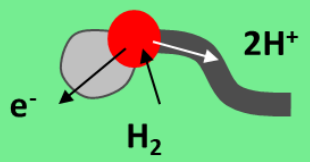

About fuel cell catalysts and electrodes

PEMFC: Electrode before adding catalyst

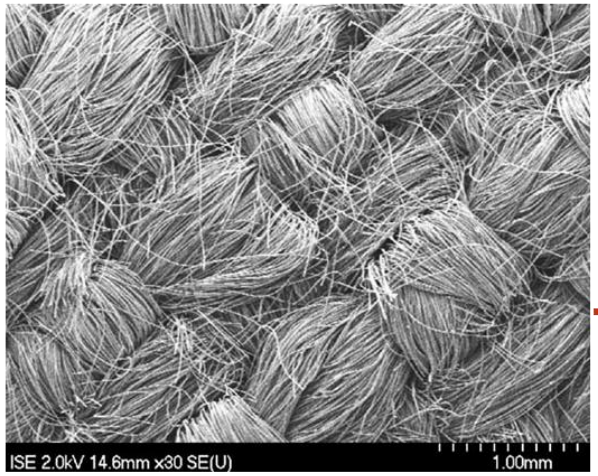

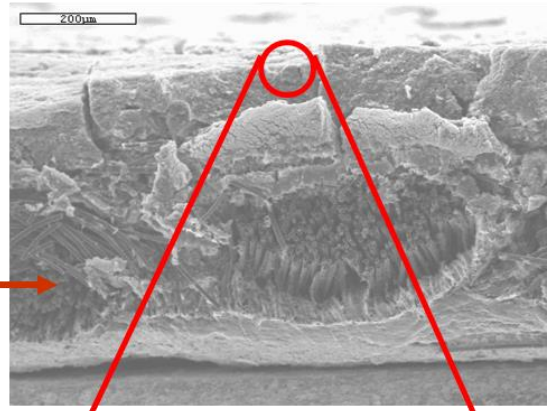

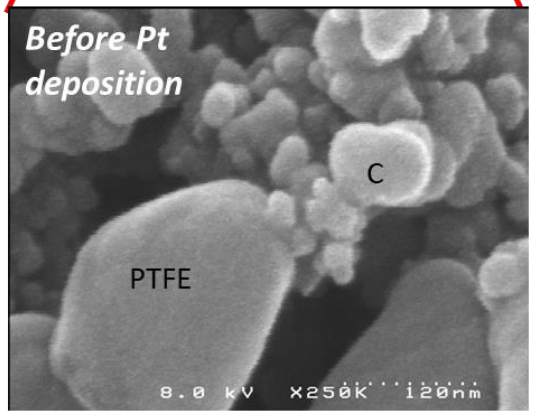

Carbon cloth : 250 m^2/g

Porous carbon : Commercial E-TEK
50 µm diffusion layer
→Ink : 80% carbon particles with 20% PTFE $(-CF_2-)_n$ painted on carbon cloth.

Porosity = 50%
ϕ_p = 30 – 100 nm
ϕ_{PTFE} = 100-300 nm

About fuel cell catalysts and electrodes

- Low loading issue:
  - Working on appropriate catalysts concentration profile in the porous GDL
  - Alloying with non-noble or low cost metal
- Catalyst stability issue in acidic PEMFC medium
  - Pt alloying
  - New corrosion resistant catalyst
- New synthesis ways for solving this issue : plasma sputtering deposition

P. Brault, *Plasma deposition of catalytic thin films: Experiments, Applications, Molecular modeling,* Surf. Coat. Technol. **205** (2011) S15-S23
P. Brault, A. Caillard, A. L. Thomann*, Polymer electrolyte fuel cell electrodes grown by vapor deposition techniques*, Chemical Vapor Deposition **17** (2011) 296-304
P. Brault, *Review of low pressure plasma processing of proton exchange membrane fuel cell electrocatalysts*, Plasma Process. Polym. **13** (2016) 10-18

Plasma sputtering insights

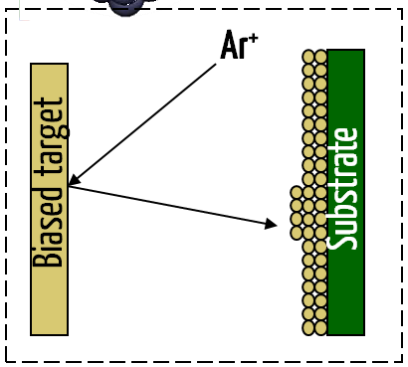

- Sputtering control (at the target)
  - Ion kinetic energy, mass, flux
- Deposition Control (at the substrate)
  - Kinetic energy, mass, flux of ions
  - Kinetic energy, mass, flux and state of active species impinging the substrate

↓

Control of: "cluster" morphology, organization, density, adhesion, ...

Sputtered Pt atom
Energy Distribution Function

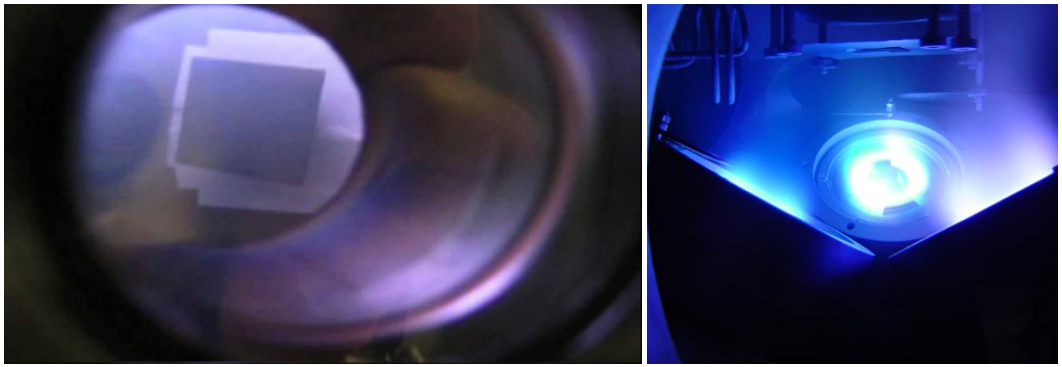

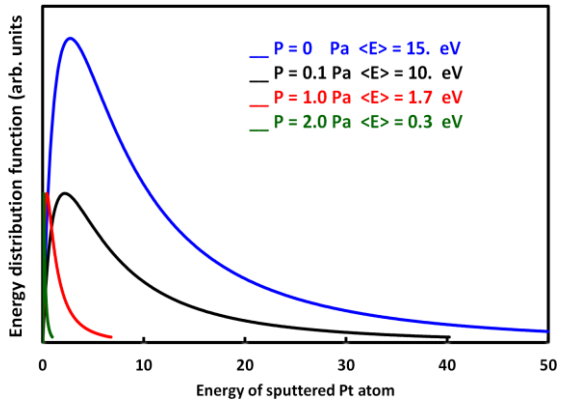

Plasma sputtering insights

- Which plasma sources ?
  - Conventional magnetron or ICP
  - HiPIMS
  - Magnetron gas aggregation nanocluster source

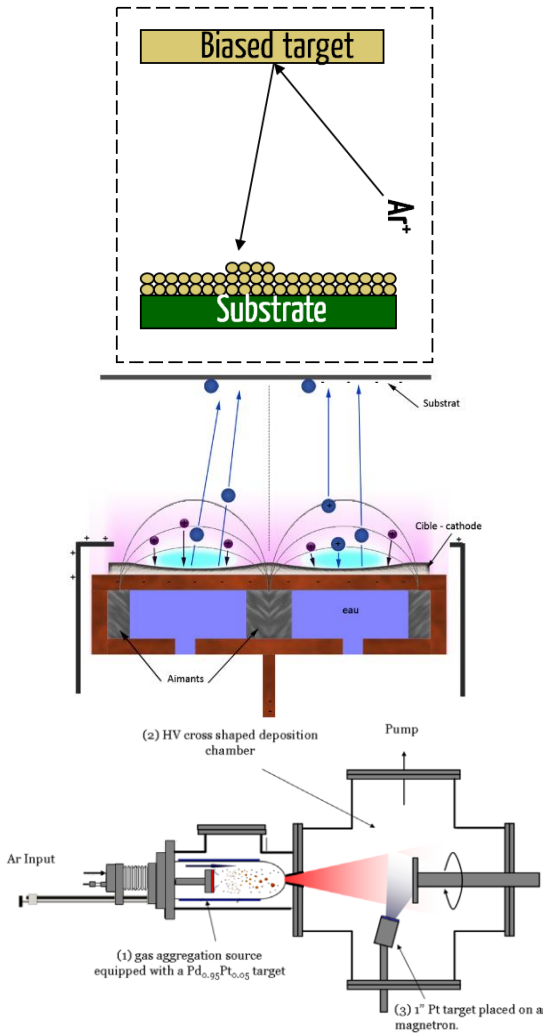

DC Magnetron sputtering of catalyst for fuel cells

- DCMS acts as an atom source
- Deposition in porous carbon electrode
  - Concentration profil management
  - Cluster size control
- Improved performances (V and W(j) plots)
- Limitations

DC Magnetron sputtering of catalyst for fuel cells

DCMS Pt deposition onto PEMFC microposous layer

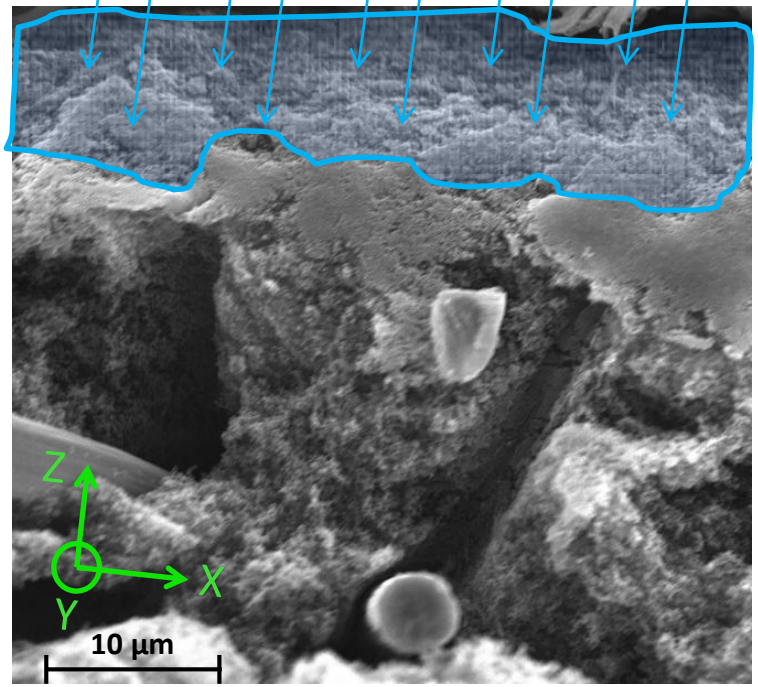

Concentration profile control : Ar pressure and substrate bias
Depth up to 400 nm

Pt clusters

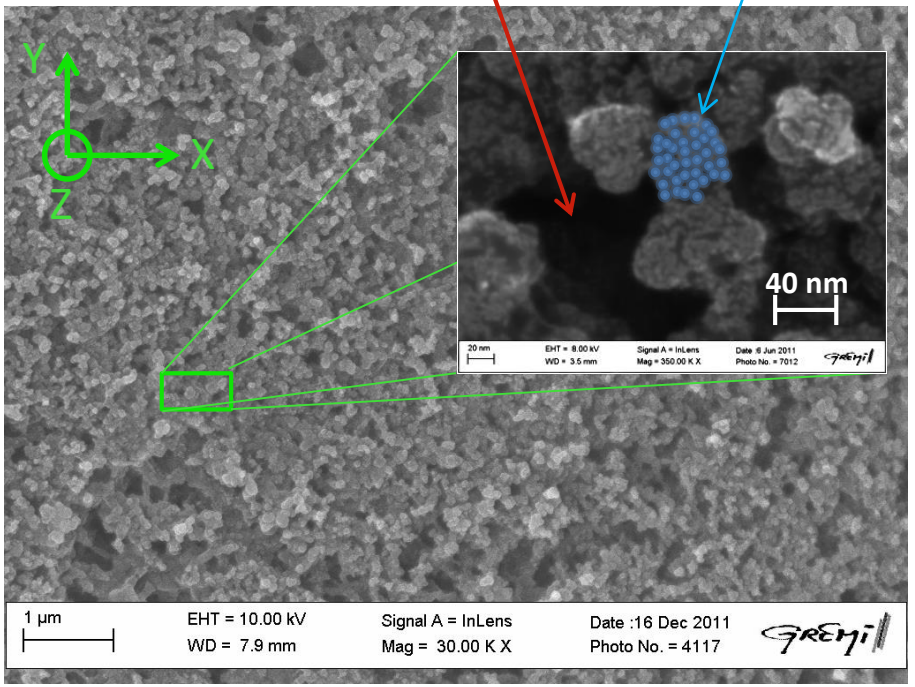

DC Magnetron sputtering of catalyst for fuel cells

PEMFC: Pt profile analyzed by RBS

Ar pressure effect

RBS Spectrum

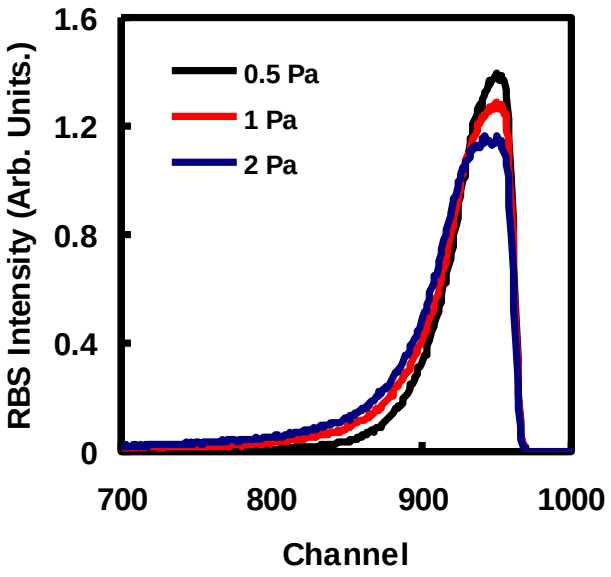

Deduced profile

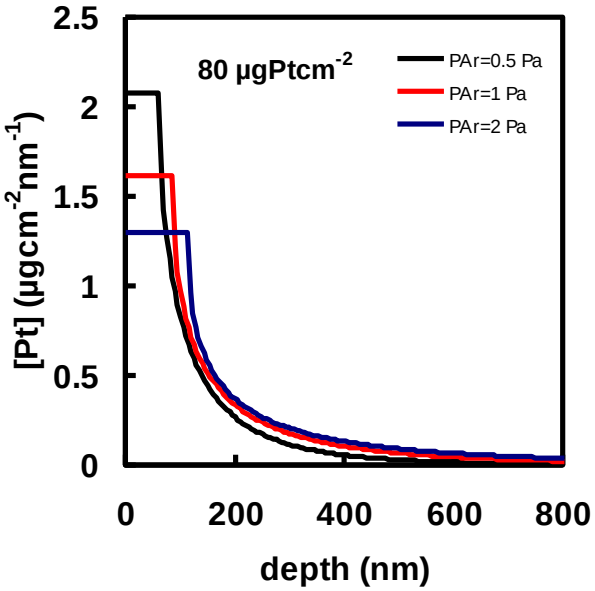

At low pressure, high superficial Pt amount and large diffusion depth

At High pressure, low constant superficial Pt amount over a large depth, more efficient diffusion pocess

DC Magnetron sputtering of catalyst for fuel cells

PEMFC: Pt profile analyzed by RBS

C cloth (substrate) bias effect

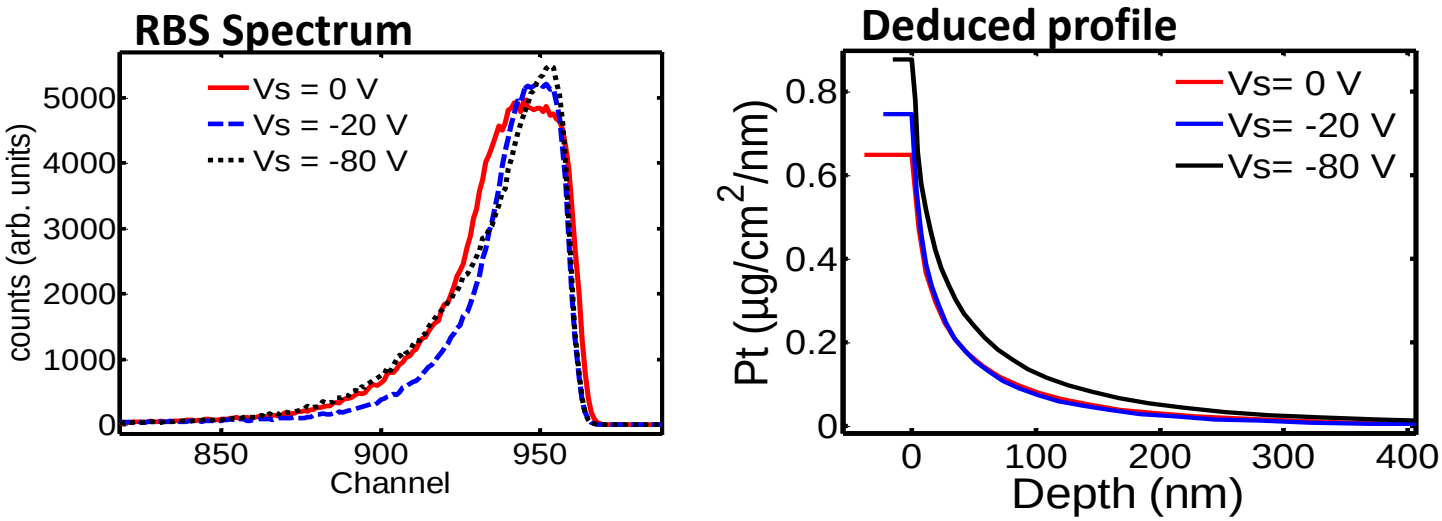

C cloth negative bias leads to profile with high Pt amount at the surface and below, over a large depth

Diffusion is assisted by attracted Ar^+ ions

- A. Caillard et al, *Deposition and diffusion of platinum nanoparticles in porous carbon assisted by plasma sputtering*, Surf. Coatings Technol. 200 (2005) 391
- A. Caillardet al, *Plasma based platinum nano-aggregates deposited on carbon nano-fibres improve fuel cell efficiency*, Appl. Phys. Lett. 90 (2007) 223119
- A. Caillard et al, *Integrated plasma synthesis of efficient catalytic nanostructures for fuel cell electrodes*, Nanotechnology 18 (2007) 305603
- P. Brault et al, *Anomalous diffusion mediated by atom deposition into a porous substrate*, Phys. Rev. Lett. 102 (2009) 045901

DC Magnetron sputtering of catalyst for fuel cells

Pt loading is significantly decreased

PVD (here magnetron) deposition allows better catalyst use.

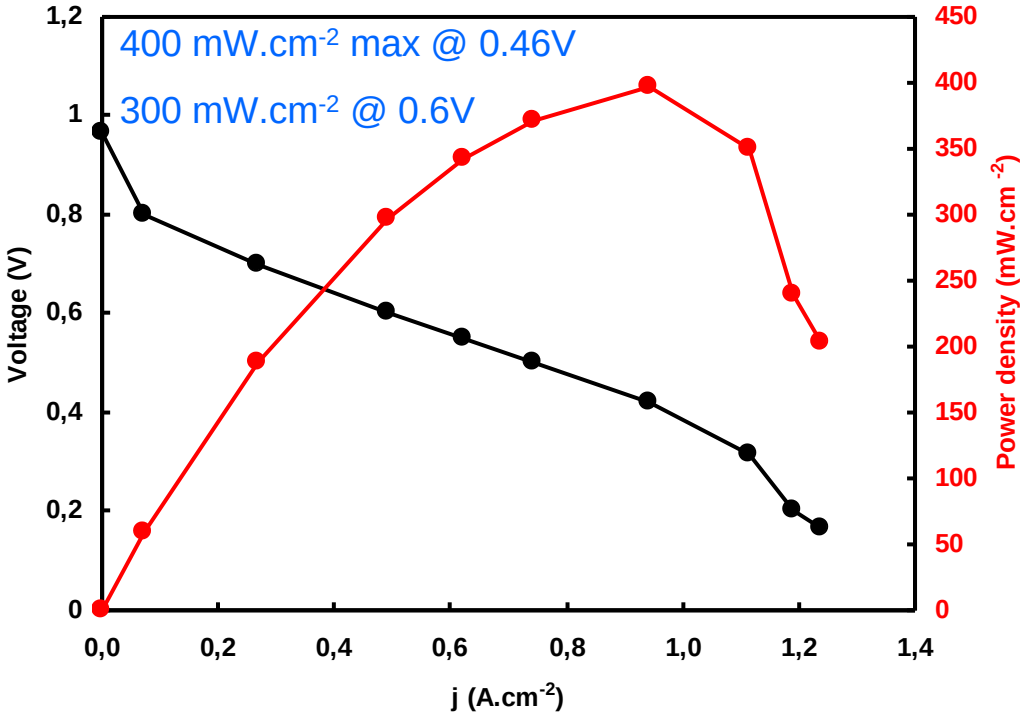

Total Pt load:0.02 mg(Pt)/cm²

Membrane : Nafion 212

Electrode: MPL E-Tech (clot)

Temperature : 80°C

Energy density **20 kW/g(Pt)**

80kW powertrain → **4g Pt**

- M. Cavarroc et al, Performance of plasma sputtered Fuel Cell electrodes with ultra-low Pt loadings, Electrochemistry Communications 11 (2009) 859 – 861

DC Magnetron sputtering of catalyst for fuel cells

Pd_9Pt_1 catalyst deposition : 10 $\mu g_{Pd9Pt1} cm^{-2}$ at both electrodes

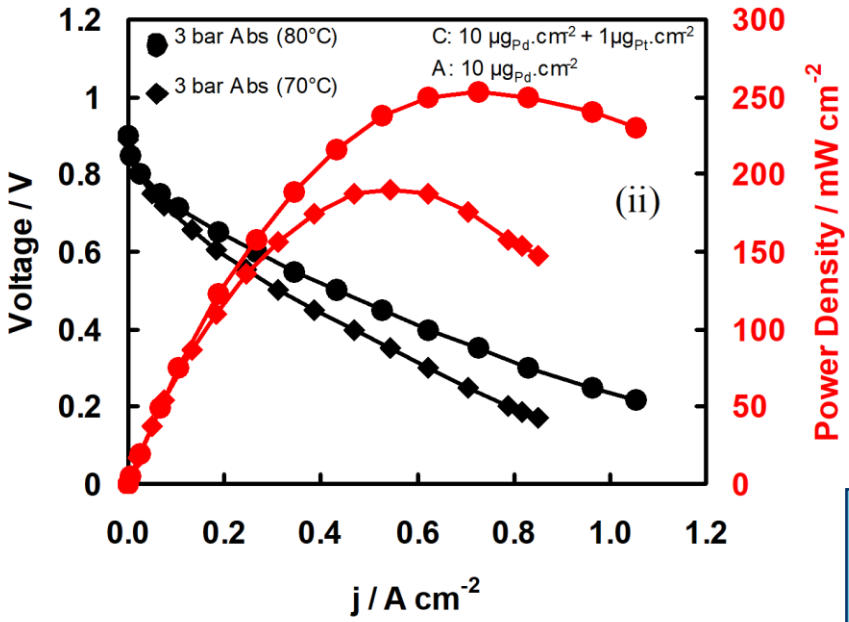

Total Pt load:0.002 mg(Pt)/cm²

Membrane : Nafion 212

Electrode: MPL E-Tech (clot)

Temperature : 80°C

Energie density 125 kW/g(Pt)

80kW powertrain → 0.6 g Pt

- M. Mougenot et al, *High Performance Plasma Sputtered PdPt Fuel Cell Electrodes with Ultra Low Loading*, International Journal of Hydrogen Energy 36 (2011) 8429-8434

DC Magnetron sputtering of catalyst for fuel cells

But ….

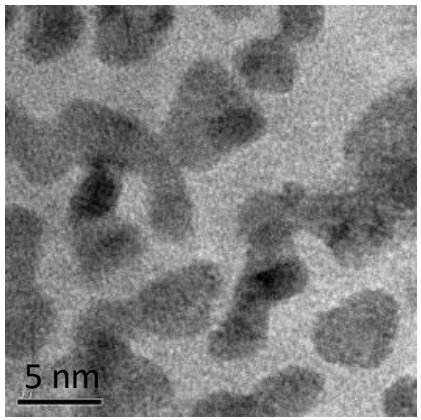

Increase of the amount of Pt catalyst deposited on the membrane

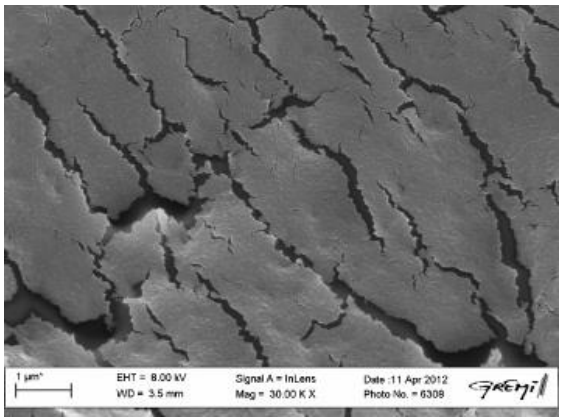

The size of the nanoclusters increase with the Pt amount

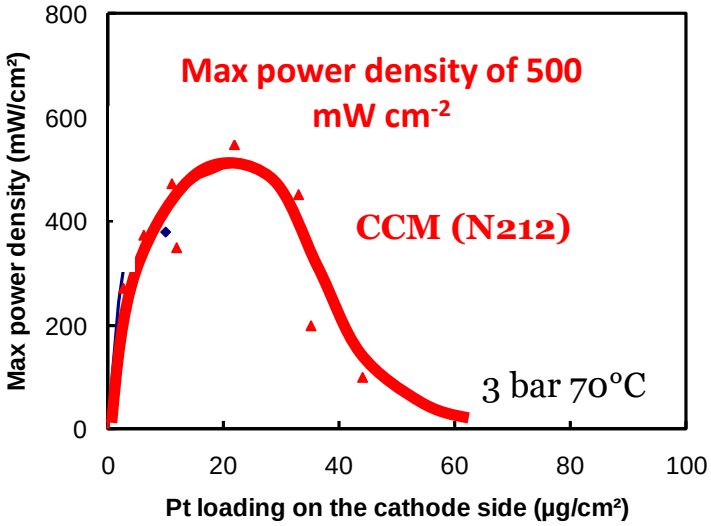

For low Pt amount:

- 3 nm in diameter Pt nanoclusters
- The aggregation of the nanoclusters starts!

For high Pt amount:

-The agglomeration of the nanocluster induce the formation of a Pt thin film.

- This dense thin film separates the GDL and the membrane.

HiPIMS

- HiPIMS : High Power Impulse Magnetron Sputtering
- Interest : High sputtered metal ion fraction

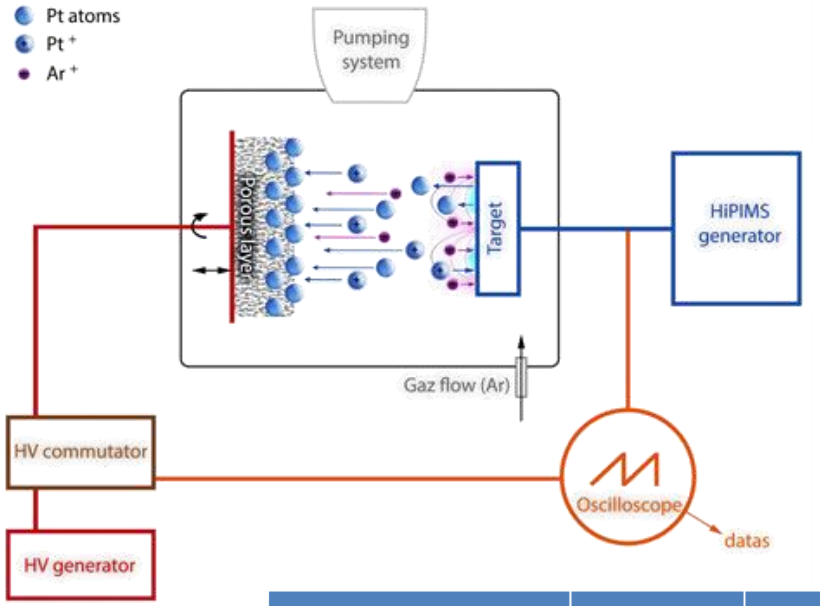

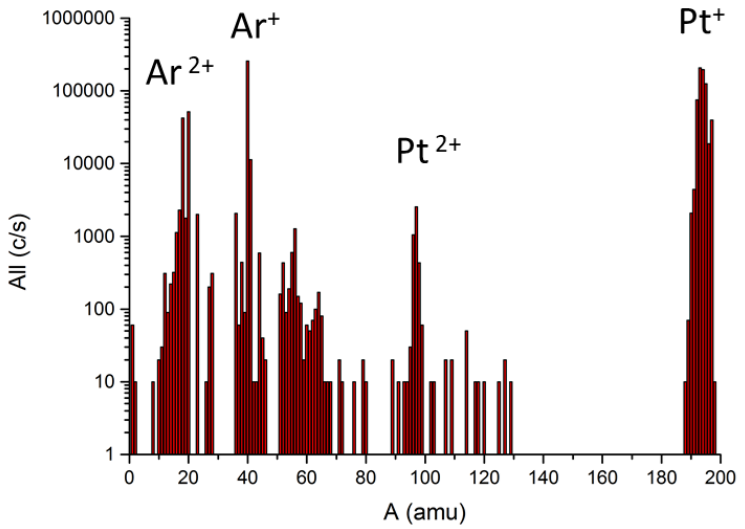

	Magnetron	Voltage (V)	Mean Power (W)	Bias	Substrate temperature	Loading (µg/cm²)
Pt/µC_DCMS	DC	500	100	Floating	RT	20
Pt/µC_DCMS400	DC	500	100	Floating	400°C	20
Pt/µC_HiPIMS1	HiPIMS	1500	100	Floating	RT	20
Pt/µC_HiPIMS_BIAS	HiPIMS	1500	100	-600 V	RT	20

HiPIMS

- Larger Pt incorparation.: comparable to DCMS 400°C
- Improved FC performances, when adding bias (-600 V) on carbon electrode

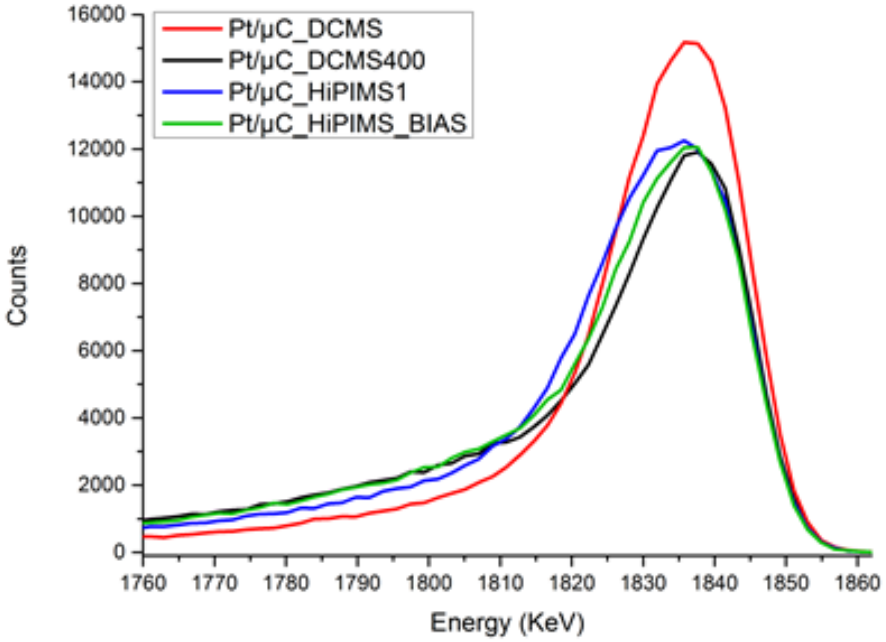

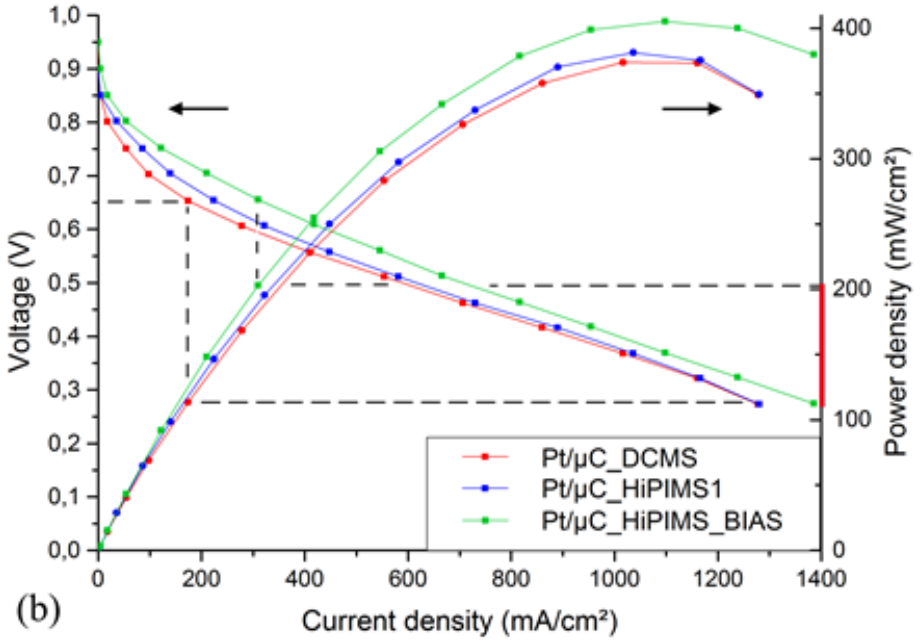

- S. Cuynet et al, *Influence of the HiPIMS voltage on the time resolved platinum ions energy distributions*, IEEE transaction on Plasma Science 42 (2014) 2818-2819.
- S. Cuynet et al, *High Power Impulse Magnetron Sputtering deposition of Pt inside fuel cell electrodes*, J. Phys. D 47 (2014) 272001
- S. Cuynet et al, *An efficient way to evidence and to measure the metal ion fraction in high power impulse magnetron sputtering (HiPIMS) post-discharge with Pt, Au, Pd and mixed targets*, Journal of Plasma Physics 82 (2016) 695820601

Magnetron gas aggregation nanocluster source

- Goal: Deposition of on-flight formed nanocatalyst
- Issues to be solved: Size distribution, deposition rate
- Principle: Sputtering in a « high » pressure (10 to 100 Pa) condensation chamber followed by transport in a differentially pumped chamber through a hole/nozzle

Magnetron gas aggregation nanocluster source

Magnetron equipped with a 2 inches target: $Pd_{0.95}Pt_{0.05}$

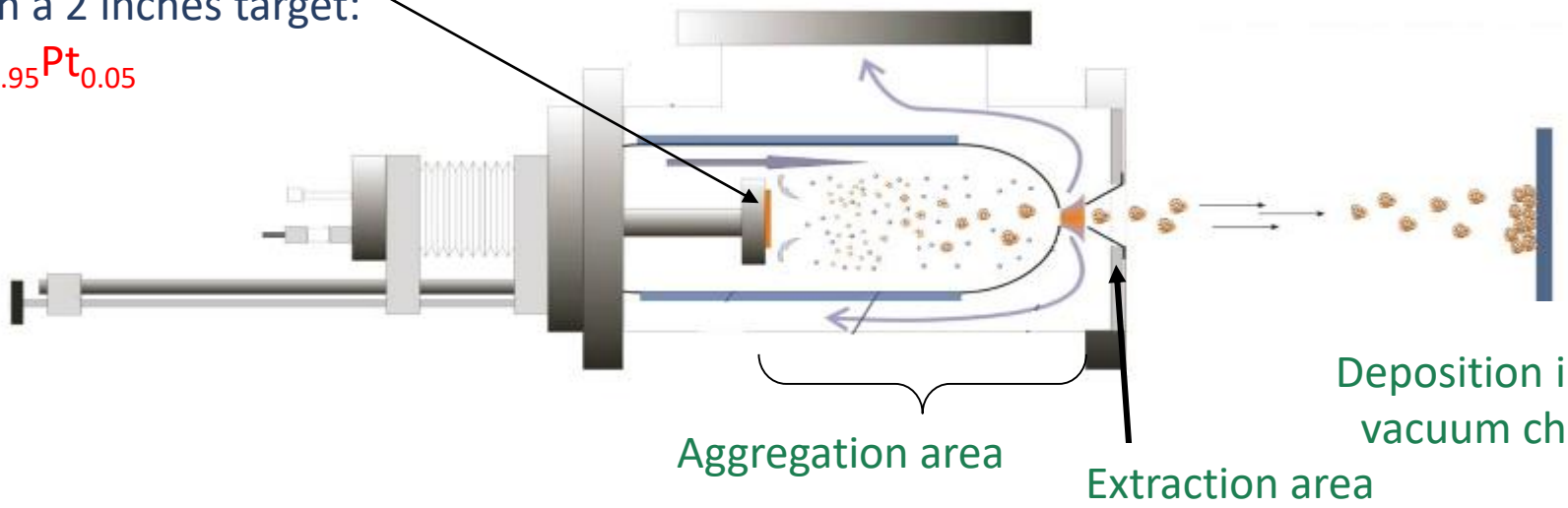

The size of the nanoclusters mainly depends on:

- The gas pressure in the aggregation area
- The length of the aggregation area

} Residence time

The amount of the nanoclusters mainly depends on:

- The gas flow carrying the nanoclusters to the extraction area
- The power applied on the target
- The pressure drop between the two chambers (in the extraction area)
- The hole/skimmer/nozzle size

Magnetron gas aggregation nanocluster source

- Growth of porous Pd thin films: nm sized Pd NPs stacking
  → Hydrogen storage ?

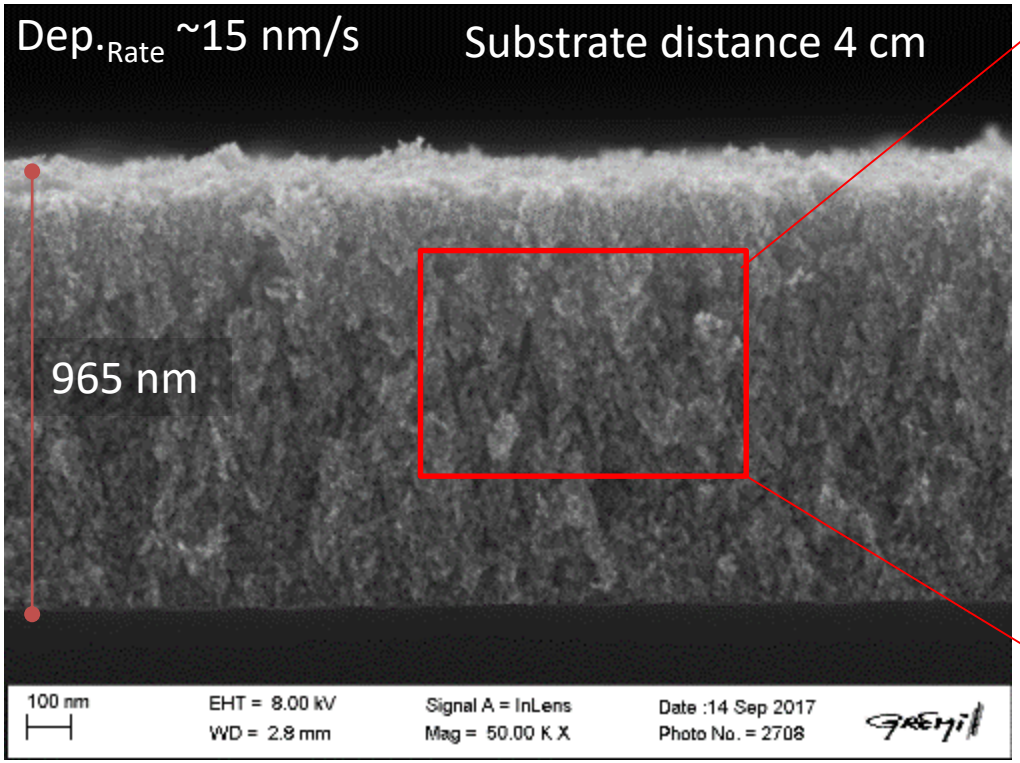

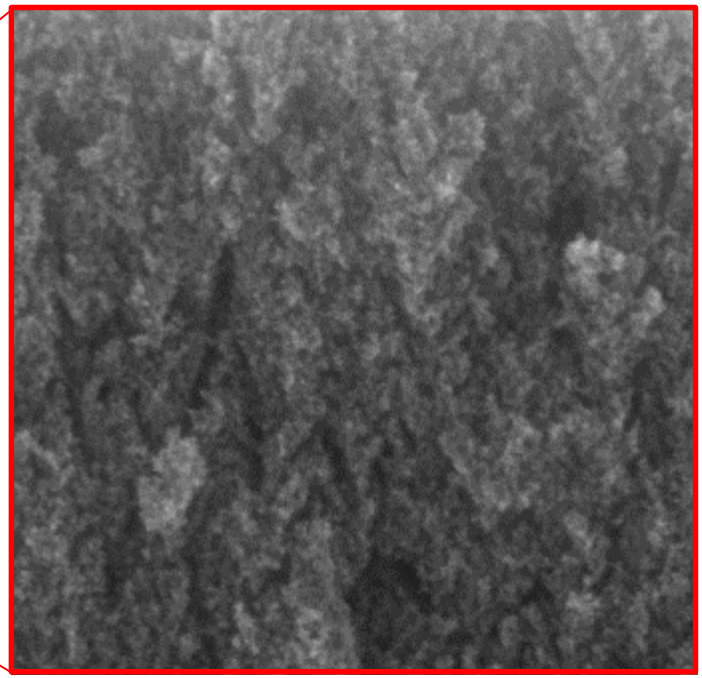

Magnetron gas aggregation nanocluster source

$Pd_{0.95}Pt_{0.05}$ nanocatalyst deposition

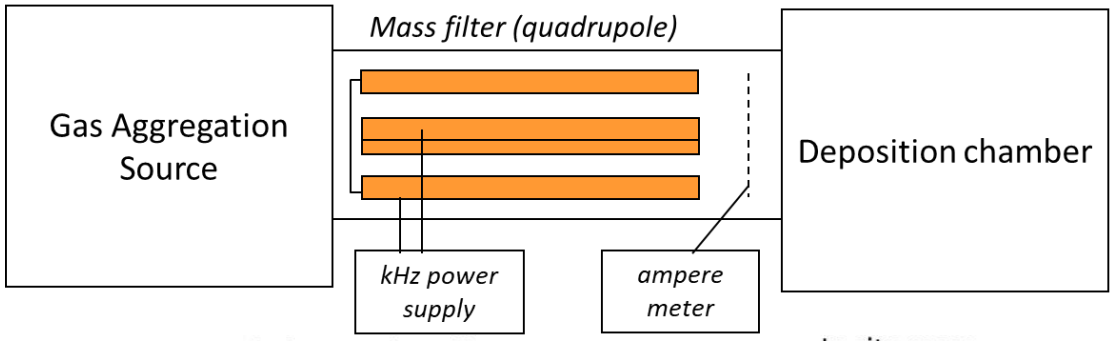

TEM analysis on carbon film

In situ mass spectrometer

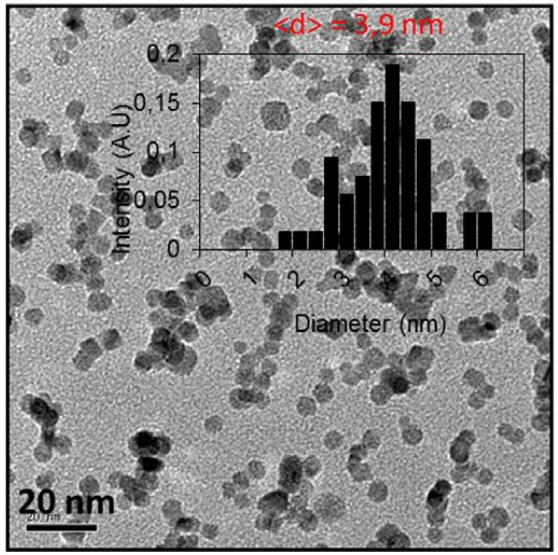

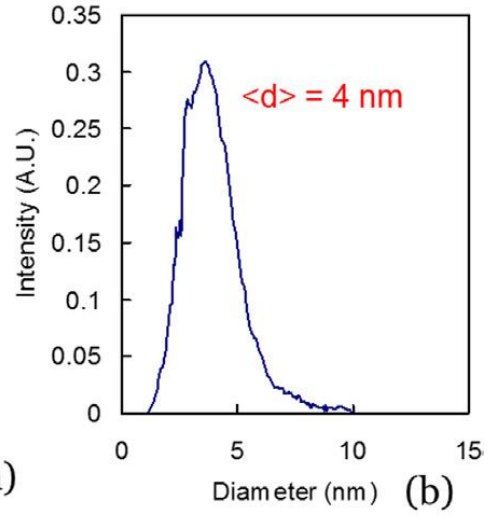

Magnetron gas aggregation nanocluster source: PdPt Catalysts

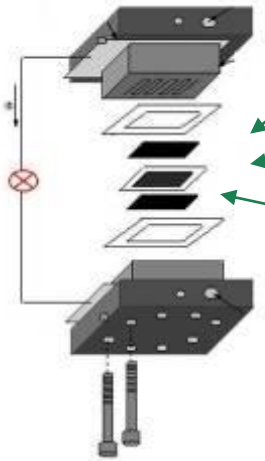

Porous carbon (gas diffusion layer)

Nafion membrane coated by PdPt nanoclusters

Porous carbon (gas diffusion layer)

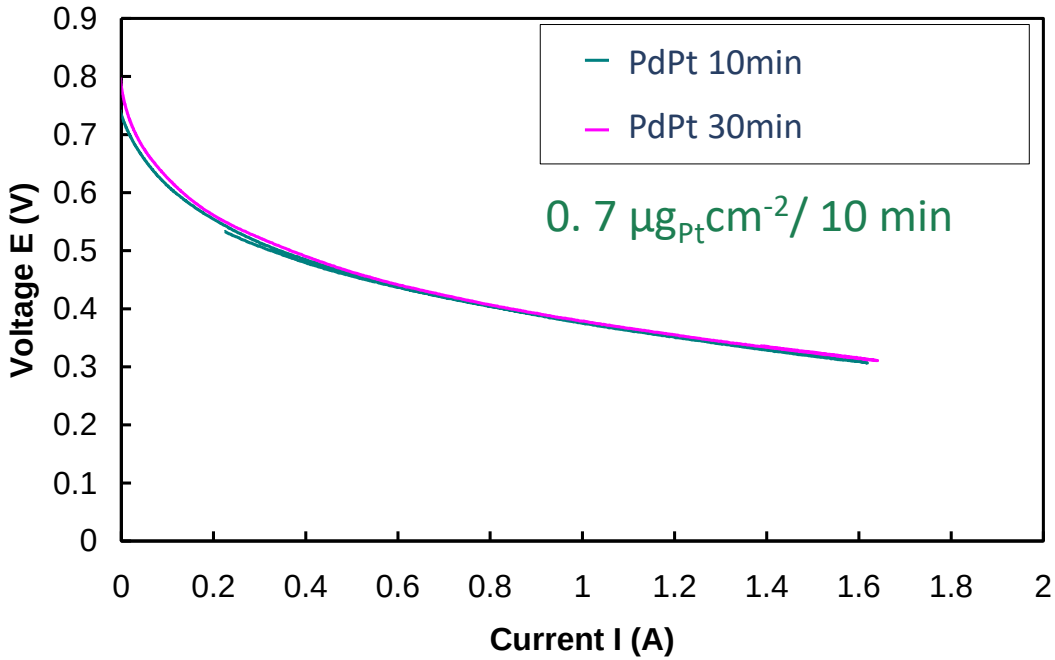

Magnetron gas aggregation nanocluster source: PdPt Catalysts

$Pd_{0.95}Pt_{0.05}$ @ Pt Core-Shell nanoclusters prepared by co-deposition (CBD & DCMS)

Alternate deposition

1/ PdPt Cluster beam deposition

2/ Pt DC magnetron sputtering

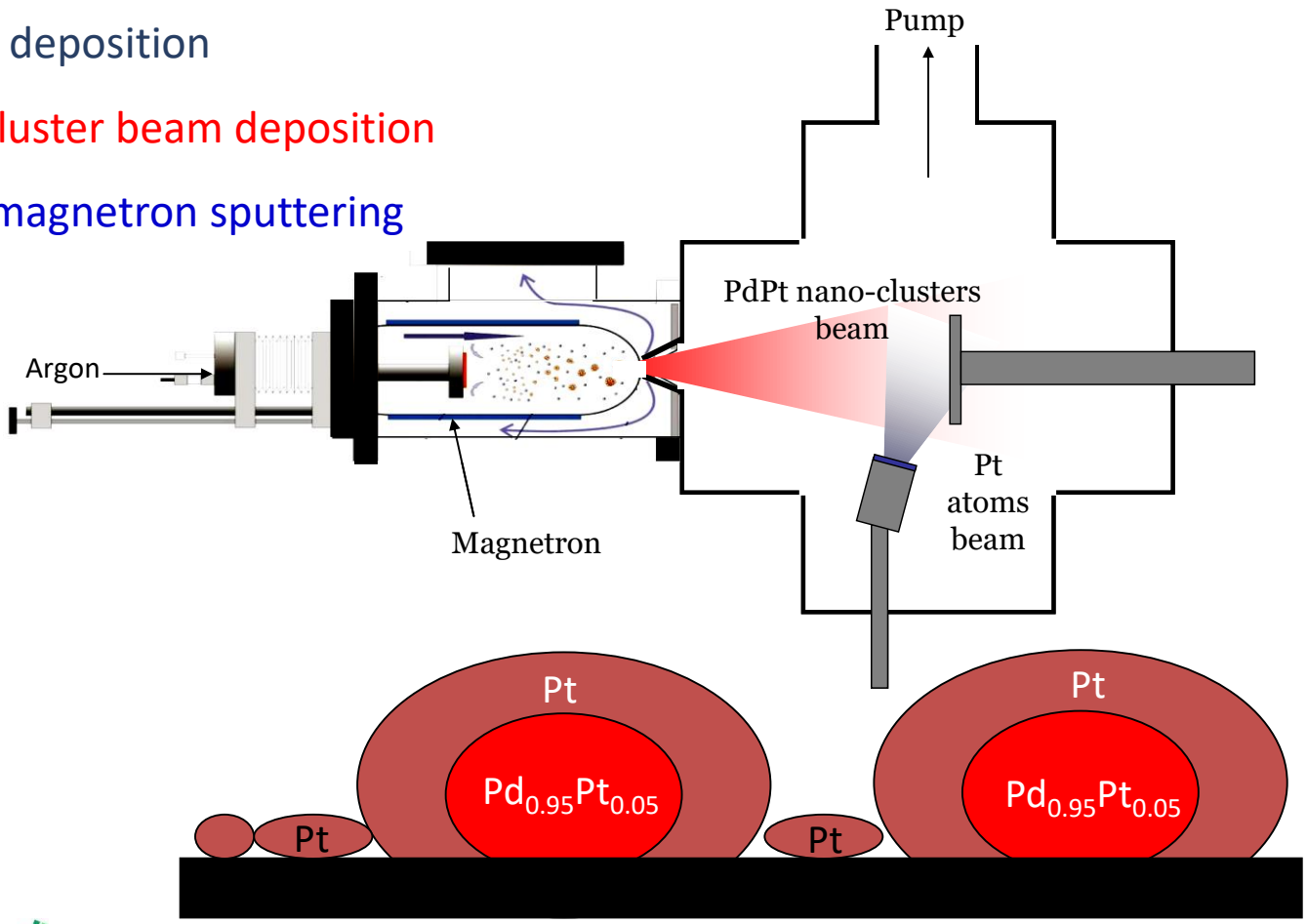

Magnetron gas aggregation nanocluster source: PdPt Catalysts

- Suitable for direct deposition on the polymer electrolyte membrane (CCM)

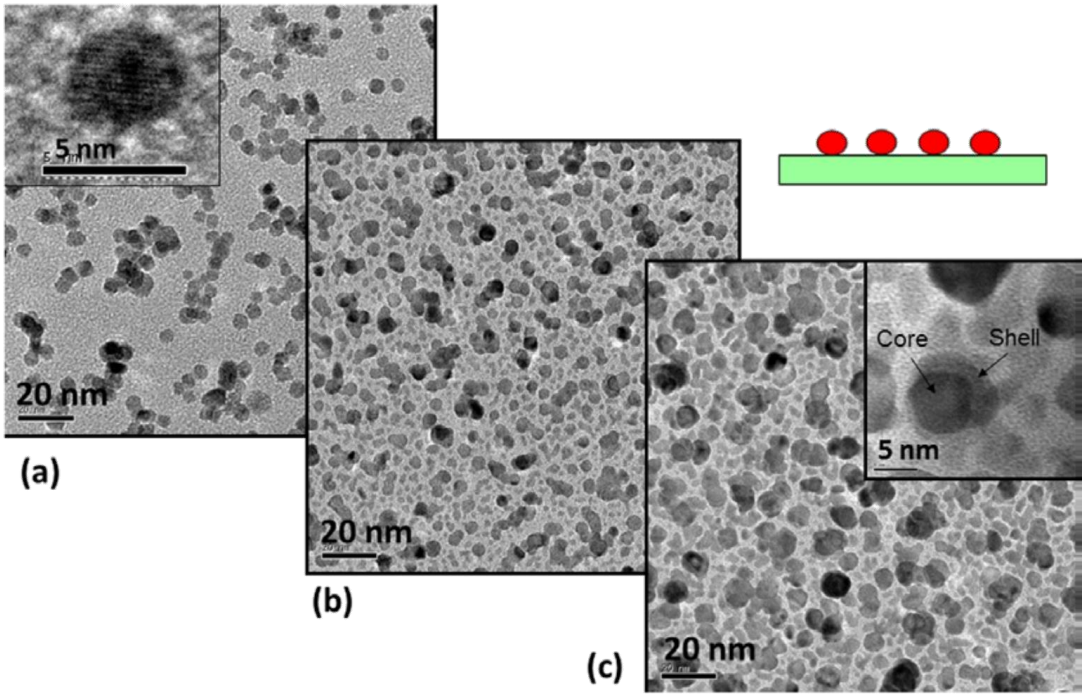

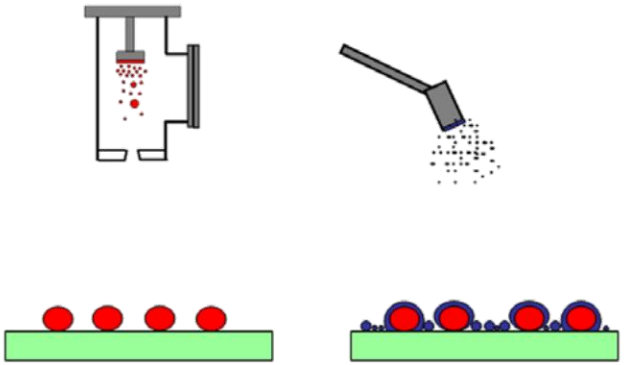

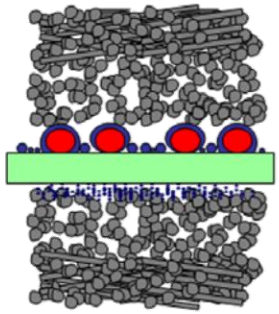

(3) PdPt@Pt coated Membrane between to two GDL

Magnetron gas aggregation nanocluster source: PdPt Catalysts

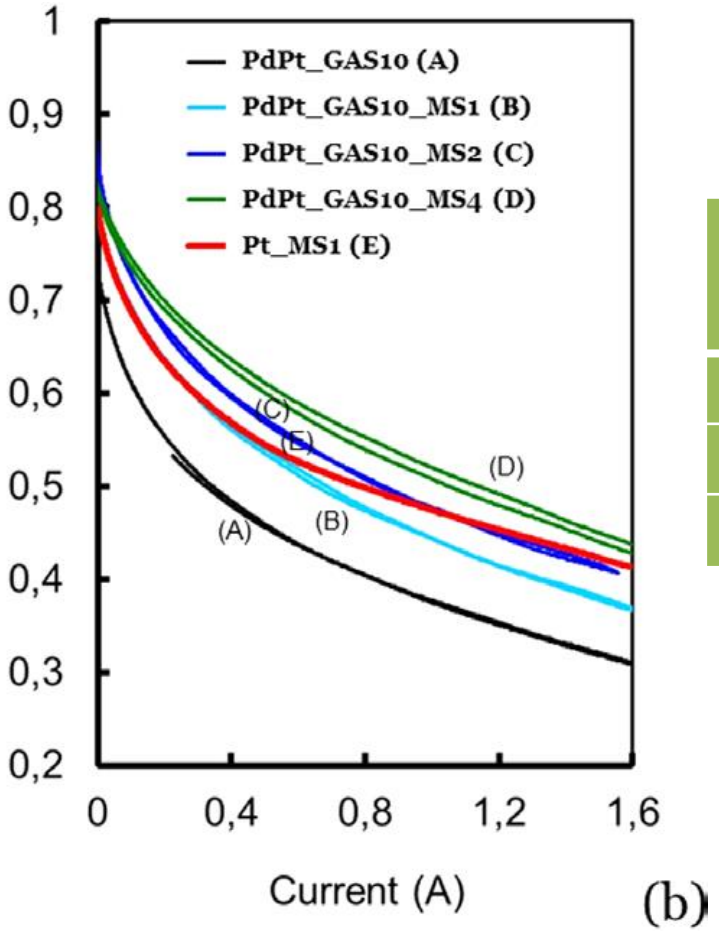

- Fuel cell tests

Name	PdPt Dep. time (min)	Pt dep. Time (min)
PdPt@Pt_GAS10_MS1	10	1
PdPt@Pt_GAS10_MS2	10	2
PdPt@Pt_GAS10_MS4	10	4

Magnetron gas aggregation nanocluster source: PdO_x Catalysts

- Growth of NPs in a reactive atmosphere: O_2 here.
- Effects of reactive atmosphere on:
  - NP size distribution
  - NP structure

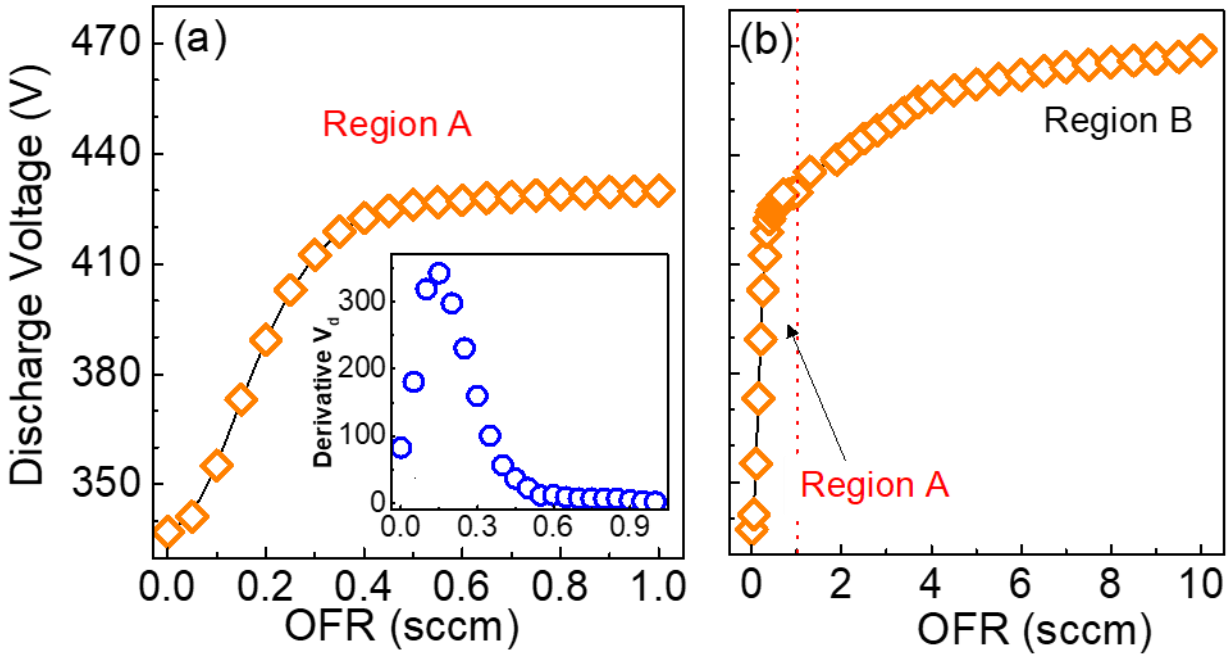

OFR: Oxygen Flow Rate

Magnetron gas aggregation nanocluster source: PdO_x Catalysts

Mass spectrometric measurement of the NP size distribution

vs

Oxygen flux and condensation distance

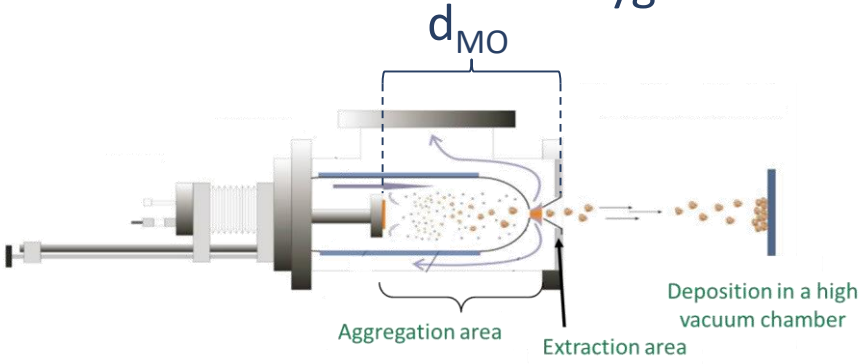

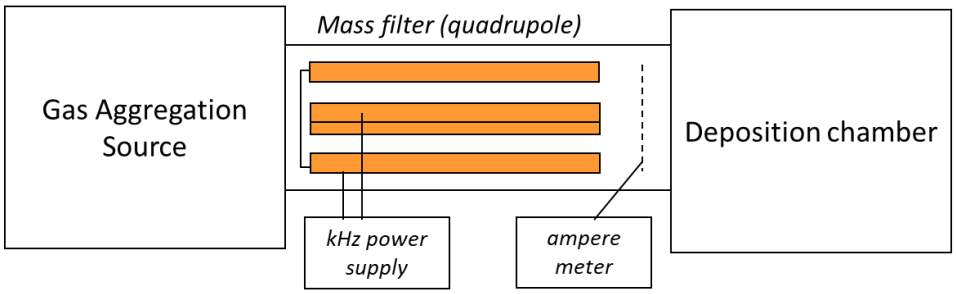

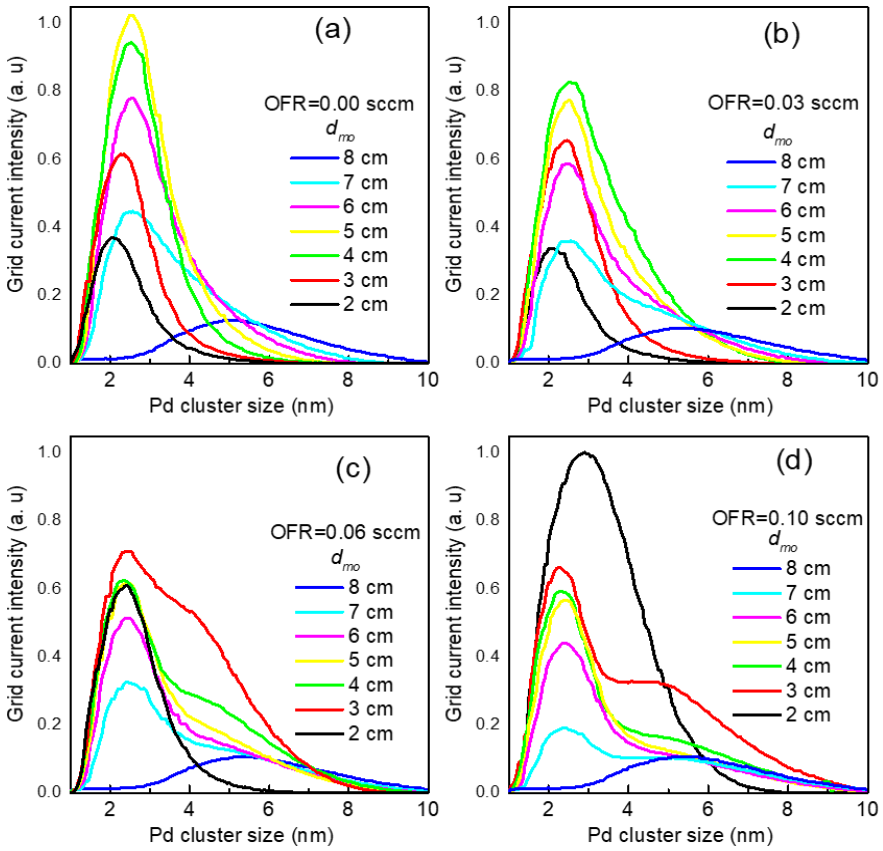

Magnetron gas aggregation nanocluster source: PdO_x Catalysts

Grazing Incidence XRD results of deposited NPs on Si(100)

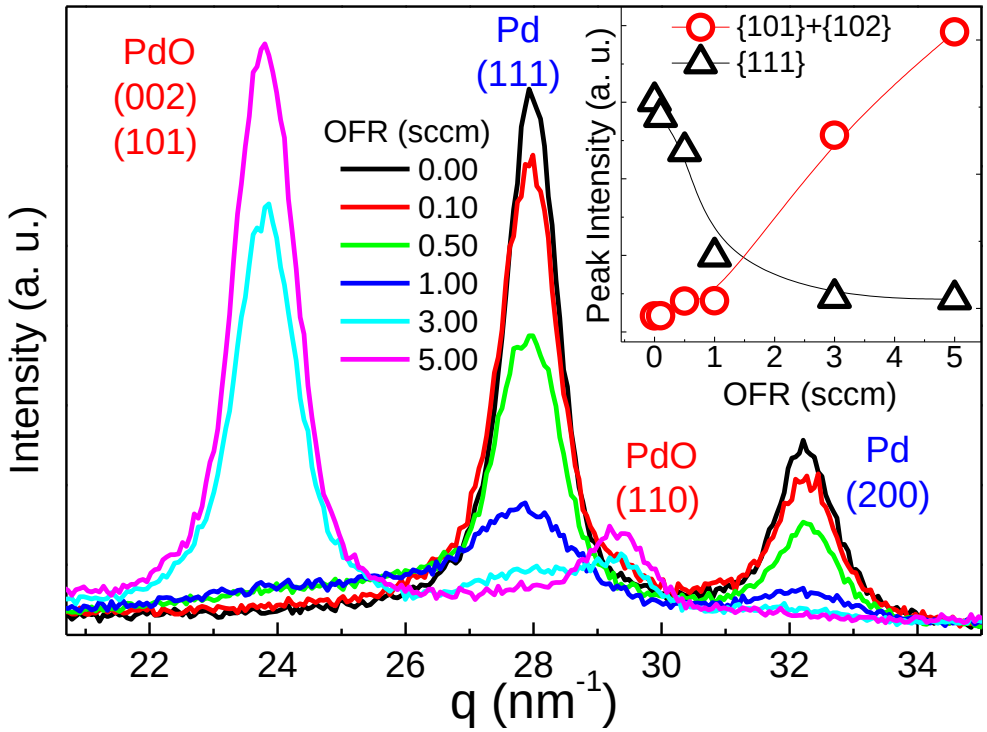

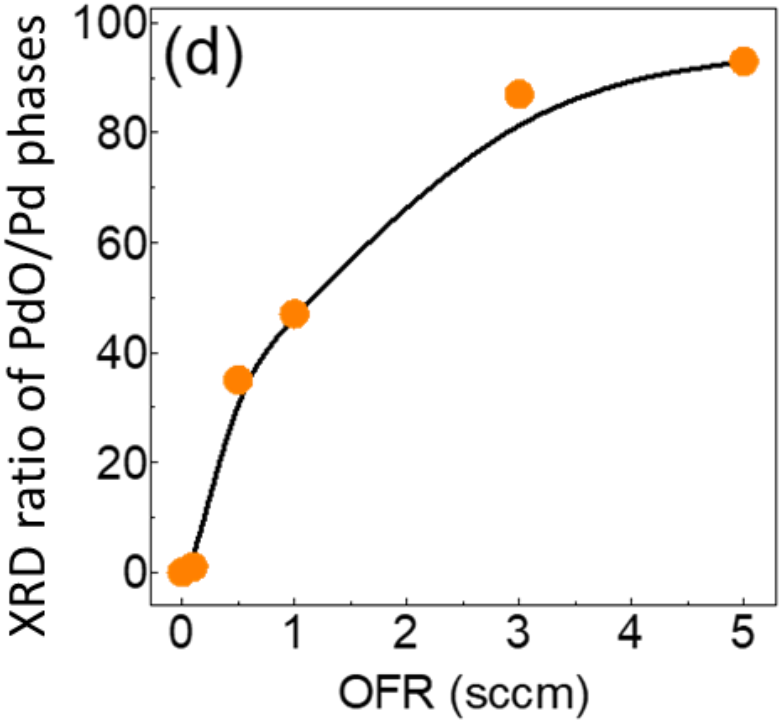

Magnetron gas aggregation nanocluster source: PdO_x Catalysts

HRTEM pictures and size distributions vs OFR

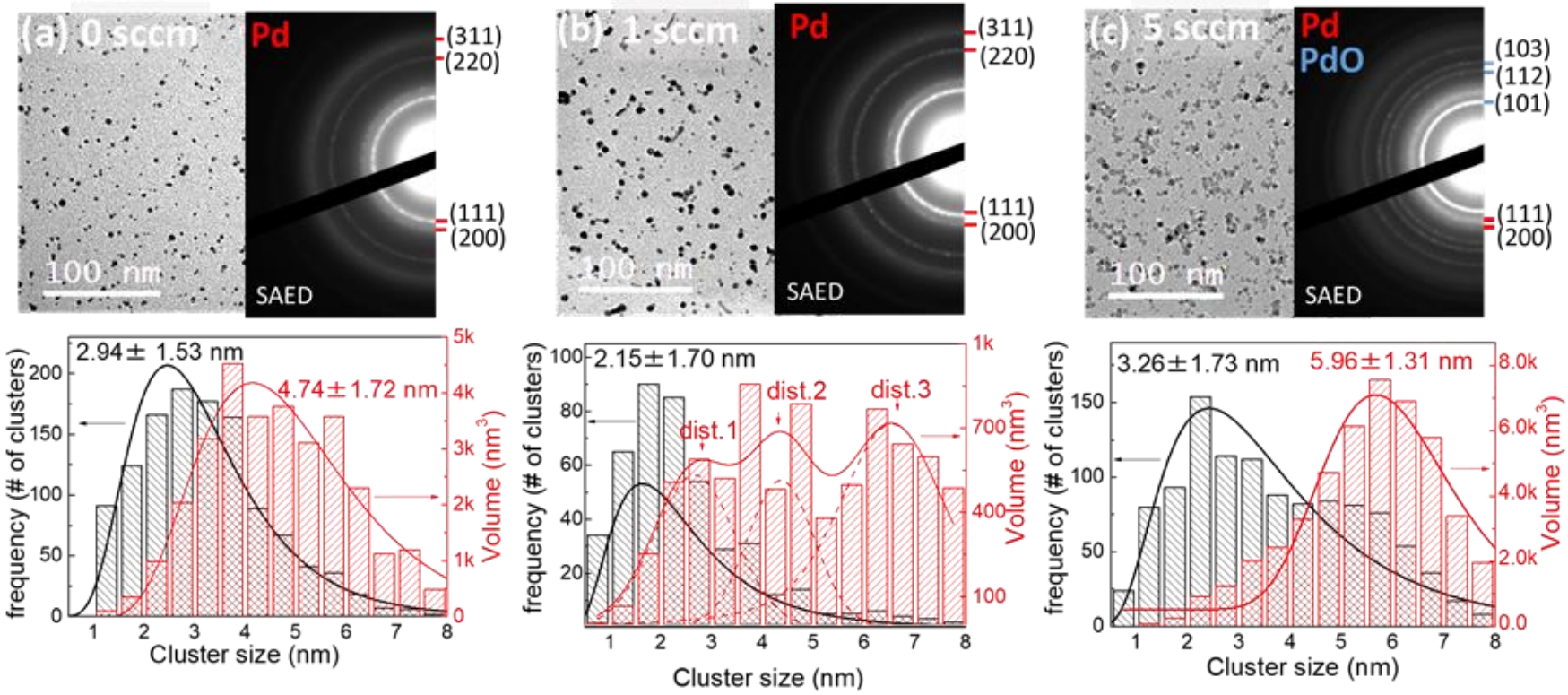

Magnetron gas aggregation nanocluster source: PdO_x Catalysts

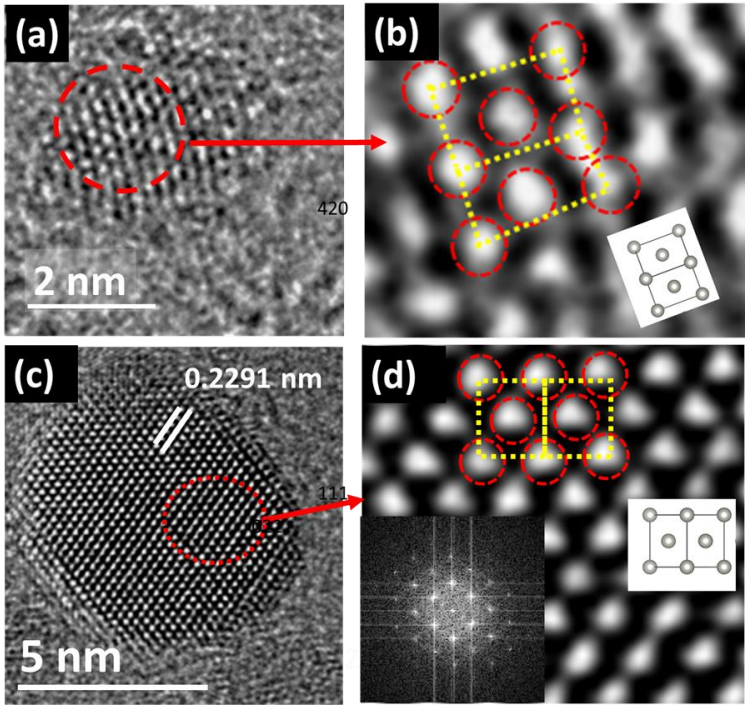

OFR = 0 sccm

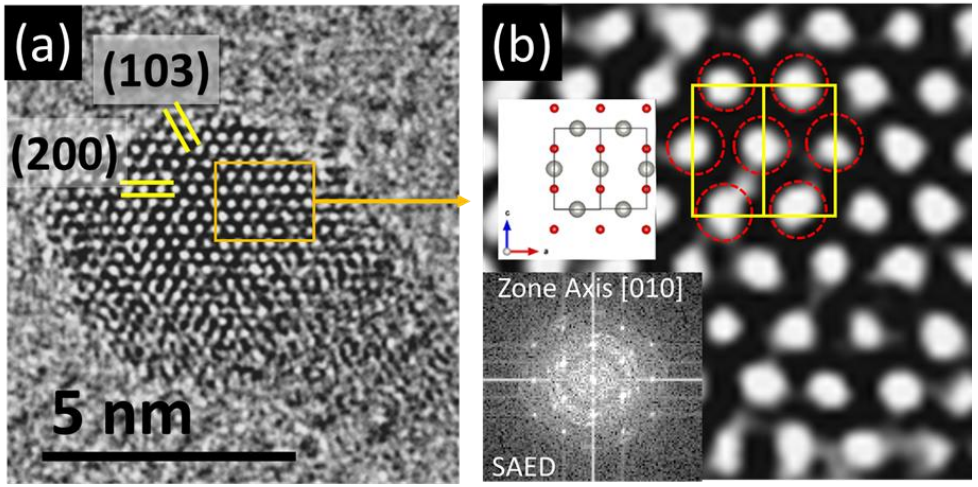

OFR = 5 sccm

Molecular dynamics simulation of sputtering plasma catalysts growth

$$\vec{F}_i = m_i \vec{a}_i = m_i \frac{d\vec{v}_i}{dt} = m_i \frac{d^2\vec{r}_i}{dt^2}$$

and

$$\vec{F}_i = -\vec{\nabla}_{ri} U\left(\vec{r}_1, \vec{r}_2, \vec{r}_3, \cdots, \vec{r}_N\right)$$

- ✓ **Calculate all trajectories of a set of atoms, molecules, ...**
  - **via the Newton equation of motion**
  - **→ Suitable for processes at nanoscale (up to 10^9 atoms)**

- ✓ **A rigourous approach requires the use of robust interaction potentials and initial conditions (positions, velocities) preferably matching experimental conditions**
  - **→ appropriate velocity distribution functions can be derived from experimental conditions.**

- ✓ **Proper energy dissipation:**
  - **Energy release during bond formation : deposition, bond formation/breaking**
  - **Annealing**
  - **→ via friction term(s), thermostat(s)**

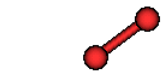

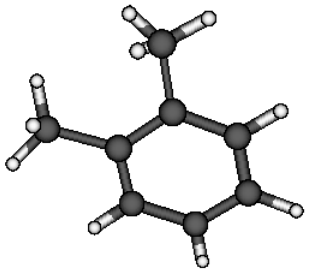

Molecular dynamics simulation of sputtering plasma catalysts growth

Relevance/significance of MD Simulations

Flux :

Exp. 1 $10^{15} cm^{-2} s^{-1}$ = 10 species / nm^2 / s - MD 1 specie /10x10 nm^2 / 2 ps

Prohibit long time diffusion, except if including specific strategies

Pressure/simulation box size

Solid density : Pt 65 nm^{-3} → Can be treated. Diffusion coefficients can be calculated without additional approximation(s)

Liquid density: water 33 nm-3

Gas density : 1 atm = 2.4 10^{-2} nm^{-3} → Not enough species in box of size d at pressure P

Solution: relevant parameter = Collision number $\propto$ P.d

→ ↑P ↓d should work.

Thermal relaxation

- Choose a relevant specie release time: i.e. greater than thermalisation time
- Choose a relevant thermostat (region i.e. what should be thermostated) within this relevant time
- For interactions with surface, one can guess that only the substrate should be thermostated

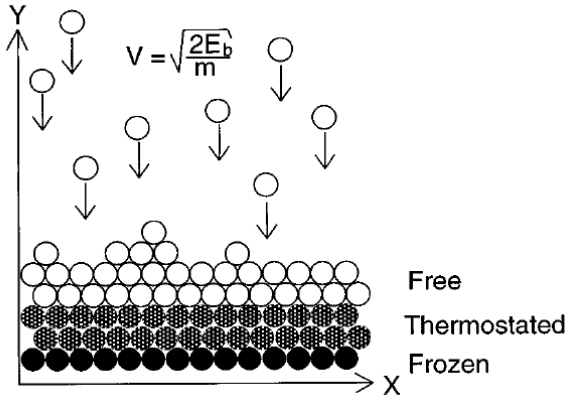

Molecular dynamics simulation of sputtering plasma catalysts growth: Interactions potentials

Metals : Embedded Atom Method (EAM)

⇒ energy of a solid is a unique functional of the electron density.

⇒ uses the concept of electron (charge) density to describe metallic bonding:

⇒ each atom contributes through a spherical, exponentially-decaying field of electron charge, centered at its nucleus, to the overall charge density of the system.

⇒ Binding of atoms is modelled as embedding these atoms in this "pool" of charge, where the energy gained by embedding an atom at location r is some function of the local density.

⇒ The total energy thus writes:

$$E_{pot} = \sum_{i=1}^{N} E_i = \frac{1}{2}\sum_{i=1}^{N}\sum_{i,j,i\neq j}^{N}\phi_{ij}(r_{ij}) + \sum_{i=1}^{N} F_i(\rho_i) \qquad \rho = \sum_{j,j\neq 1}^{N} f_i(r_{ij}) \qquad f(r) = \frac{f_e \exp\left[-\beta\left(\frac{r}{r_e}-1\right)\right]}{1+\left(\frac{r}{r_e}-\lambda\right)^{20}}$$

With pairwise function:

$$\phi(r) = \frac{A\exp\left[-\alpha\left(\frac{r}{r_e}-1\right)\right]}{1+\left(\frac{r}{r_e}-\kappa\right)^{20}} - \frac{B\exp\left[-\beta\left(\frac{r}{r_e}-1\right)\right]}{1+\left(\frac{r}{r_e}-\lambda\right)^{20}}$$

and mixing rule:

$$\phi^{ab}(r) = \frac{1}{2}\left[\frac{f^b(r)}{f^a(r)}\phi^{aa}(r) + \frac{f^a(r)}{f^b(r)}\phi^{bb}(r)\right]$$

S.M. Foiles, M.I. Baskes Contributions of the embedded-atom method to materials science and engineering, MRS Bulletin, 37 (2012) 485-491.
X. W. Zhou et al, Misfit-energy-increasing dislocations in vapor-deposited CoFe/NiFe multilayers, Phys. Rev. B 69 (2004) 144113

Molecular dynamics simulation of sputtering plasma catalysts growth: Interactions potentials

ReaxFF allows for computationally efficient simulation of materials under realistic conditions, *i.e.* bond breaking and formation with accurate chemical energies. It also includes variable partial charges.

Due to the chemistry, ReaxFF has a complicated potential energy function: $E_{system} = E_{bond} + E_{over} + E_{angle} + E_{tors} + E_{vdWaals} + E_{Coulomb} + E_{Specific}$

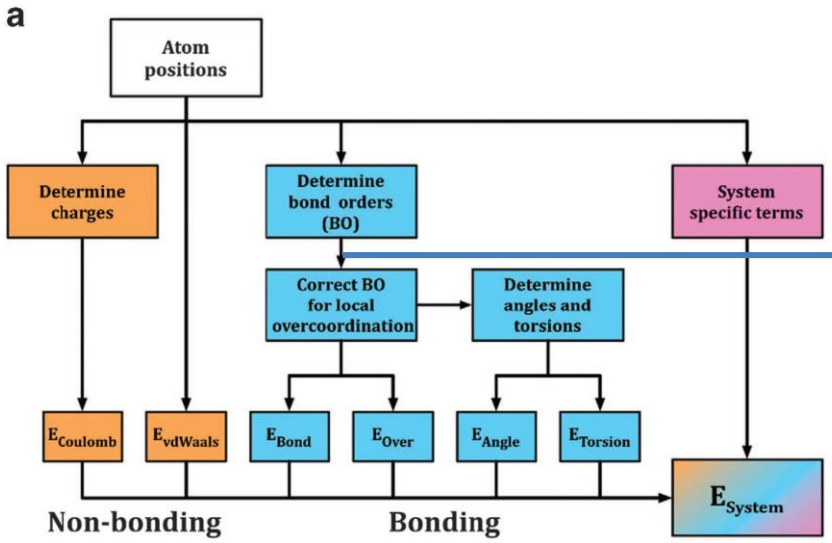

Overview of the ReaxFF total energy components

$$BO_{ij} = BO_{ij}^{\sigma} + BO_{ij}^{\pi} + BO_{ij}^{\pi\pi}$$
$$= \exp\left[p_{bo1}\left(\frac{r_{ij}}{r_o^{\sigma}}\right)^{p_{bo2}}\right] + \exp\left[p_{bo3}\left(\frac{r_{ij}}{r_o^{\pi}}\right)^{p_{bo4}}\right]$$
$$+ \exp\left[p_{bo5}\left(\frac{r_{ij}}{r_o^{\pi\pi}}\right)^{p_{bo6}}\right]$$

Correct Bond Order ⇒ Correct description of reaction energy barriers

TP Senftle et al, *The ReaxFF reactive force-field: development, applications and future directions*, npj Computational Materials 2, (2016) 15011

Molecular dynamics simulation of sputtering plasma catalysts growth: Supported Pt_2PdAu nanocatalyst growth on porous carbon

Potentials used in the system:

Pt-Pd-Au: EAM potentials

C – C: Tersoff potential -> thermostat

Metal – C: LJ potential (Steele)

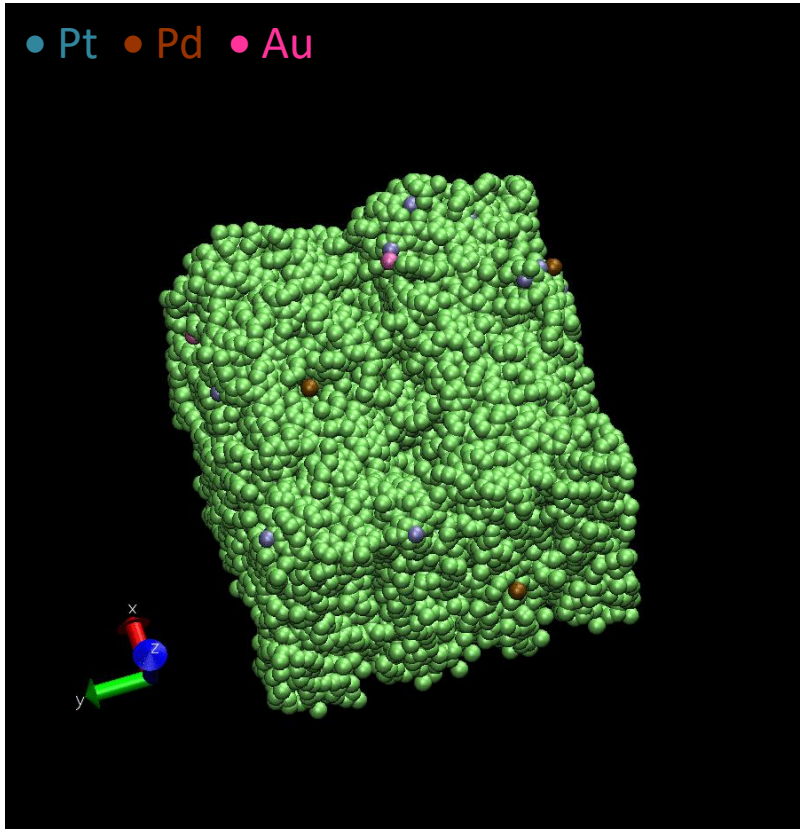

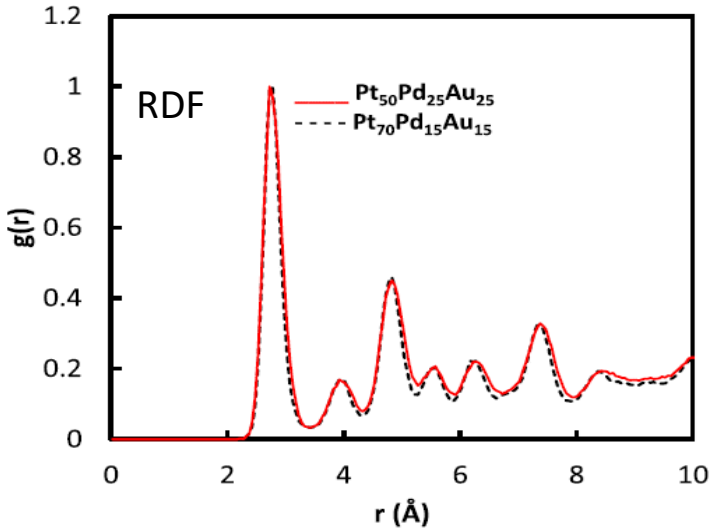

Table 1 – EAM and average experimental surface energies of the low index faces of Pt, Pd, Au in Jm^{-2} [40].

	Pt	Pd	Au
(111)	1.44	1.22	0.79
(100)	1.65	1.37	0.92
(110)	1.75	1.49	0.98
Experimental, face averaged	2.49	2.00	1.5

- Gold surface segregation

Molecular dynamics simulation of sputtering plasma catalysts growth: Supported Pt_2PdAu nanocatalyst growth on porous carbon

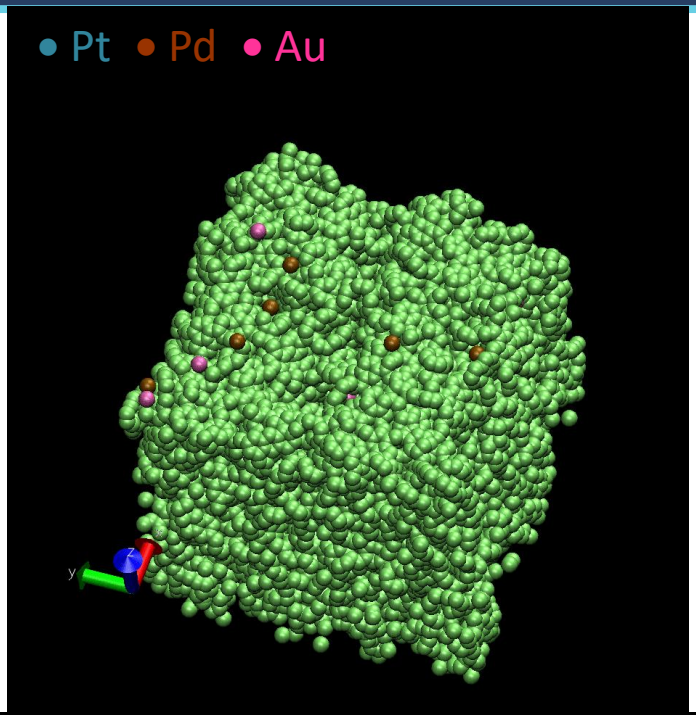

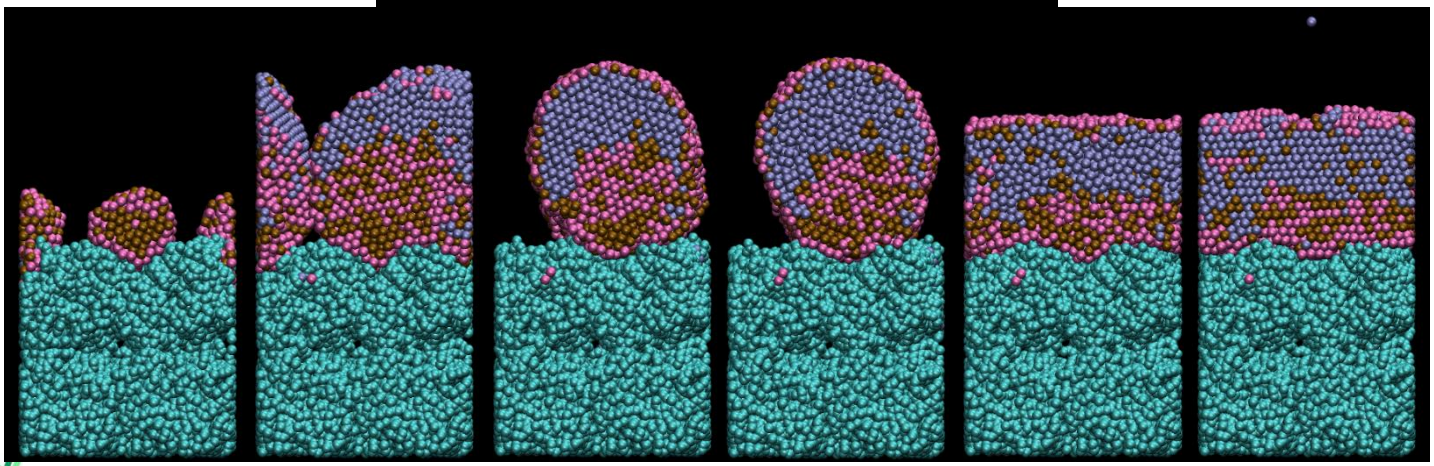

Molecular dynamics simulation of sputtering plasma catalysts growth: Supported Pt_2PdAu nanocatalyst growth on porous carbon

Correlations between cluster temperature evolution and morphology transform in the course of deposition of core-shell $PdAu@Pt_2$ nanocatalyst

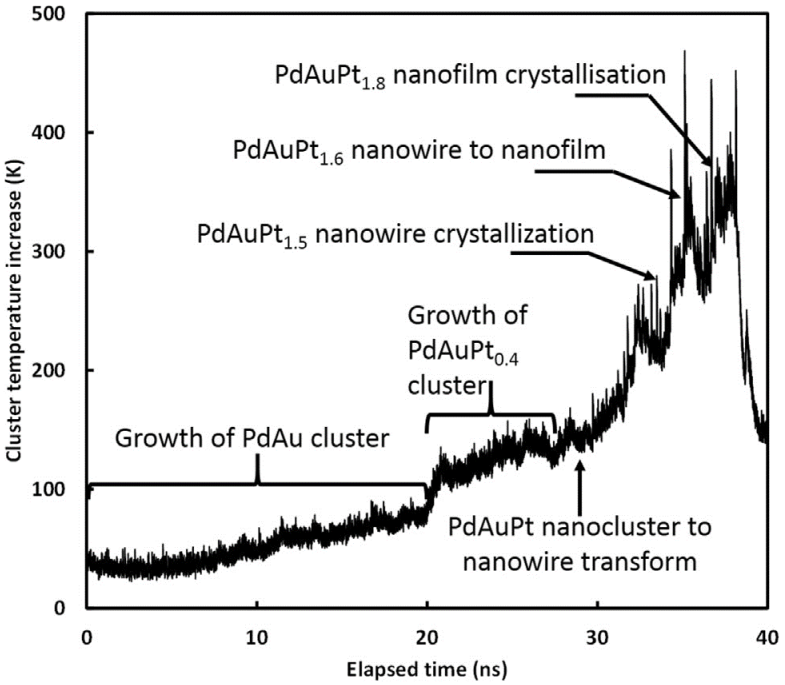

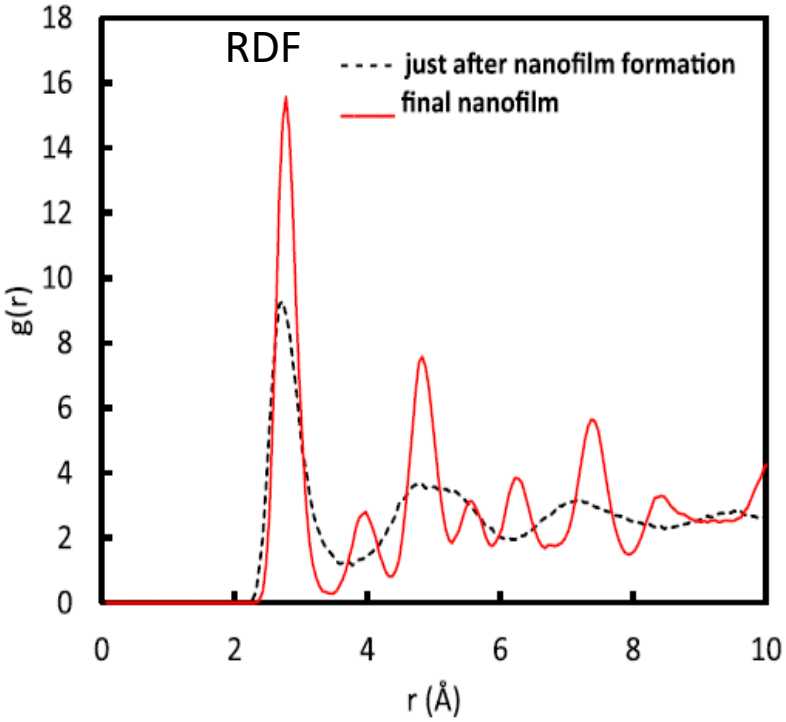

- L. Xie, P. Brault, C. Coutanceau, A. Caillard, J. Berndt, E. Neyts Appl. Cat. B, 62 (2015) 21 – 26
- P. Brault, C. Coutanceau, P. C. Jennings, T. Vegge, J. Berndt, A. Caillard, S. Baranton, S. Lankiang, International Journal of Hydrogen Energy 41 (2016) 22589-22597
- E. Neyts, P. Brault, Plasma Processes and Polymers 14 (2017) 1600145 (Review article)
- FP7 FCH-JU SMARTCat project #325327

Molecular dynamics simulation of sputtering plasma catalysts growth: Free Pt_3NiAu nanocatalyst growth

Gas aggregation source: simulation principles

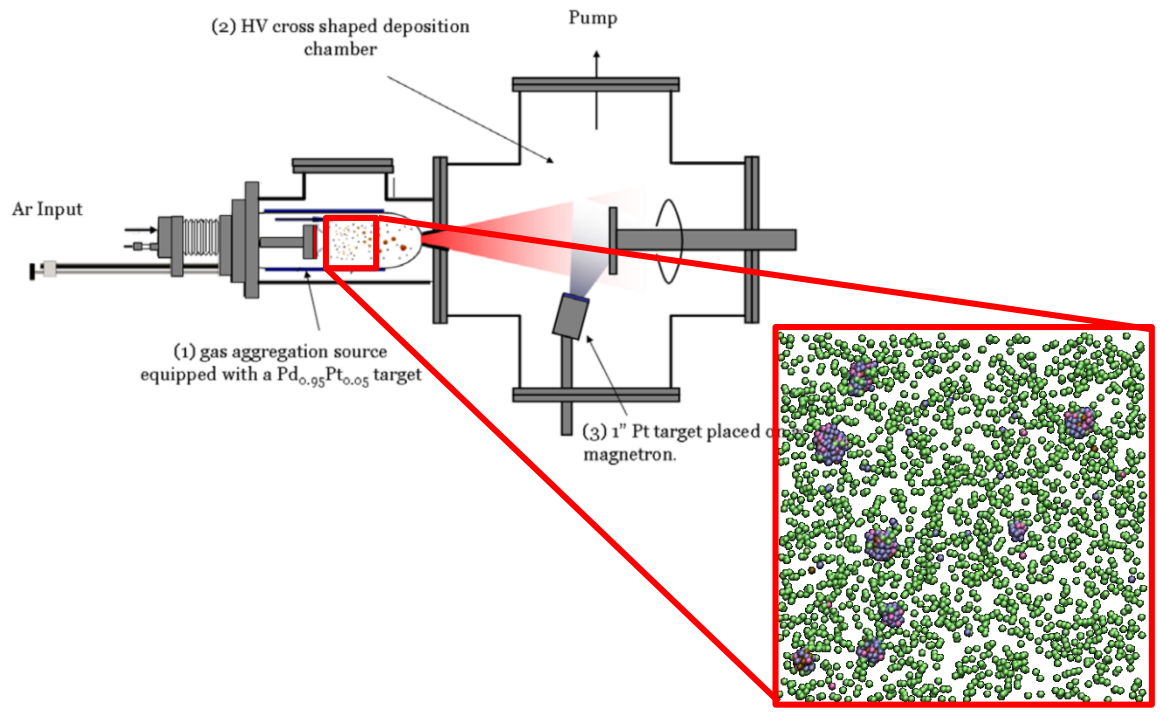

Matching experimental and simulation conditions

- Metal vapor density in the aggregation chamber

$N_M = (Y_{Ar}\, I / q) / (\Phi(Ar).P_{at} / P_{Ar})$

→ will give the proper ratio of N_M/N_{Ar} in the simulation box

- Collision number identical in experiments and in simulation

i.e. $P_{exp}.d_{exp} = P_{sim}.d_{sim}$

A. Caillard et al, *PdPt catalyst synthesized using a gas aggregation source and magnetron sputtering for fuel cell electrodes*, J. Phys. D: Appl. Phys. 48 (2015) 475302

E Quesnel et *al Modeling metallic nanoparticle synthesis in a magnetron-based nanocluster source by gas condensation of a sputtered vapor*, J. Appl. Phys. 107 (2010) 054309

Molecular dynamics simulation of sputtering plasma catalysts growth: Free Pt_3NiAu nanocatalyst growth

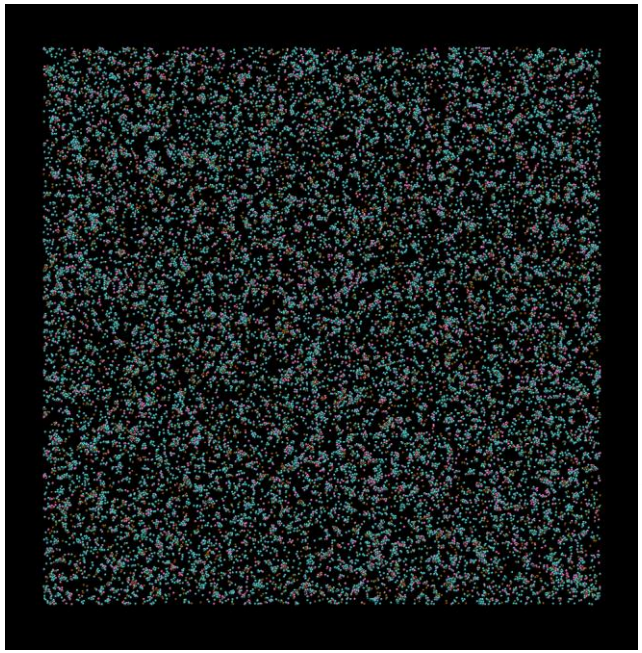

Tricks :

NVE ensemble for Pt, Ni and Au

NVT ensemble for Ar : surrounding gas is the thermostat

Ratio of N_{Ar} to N_{metal} estimated from experiments: depends on discharge current, Ar pressure, …

here: N_{Ar}=128000; N_{Pt}=19200; N_{Ni}=6400; N_{Au}=6400

Box size 64x64x64 nm^3

Temperature evolution of the vapor and of the metal vapor and then clusters display the cluster growth and coalescence : breaks in the plot (green vertical sticks)

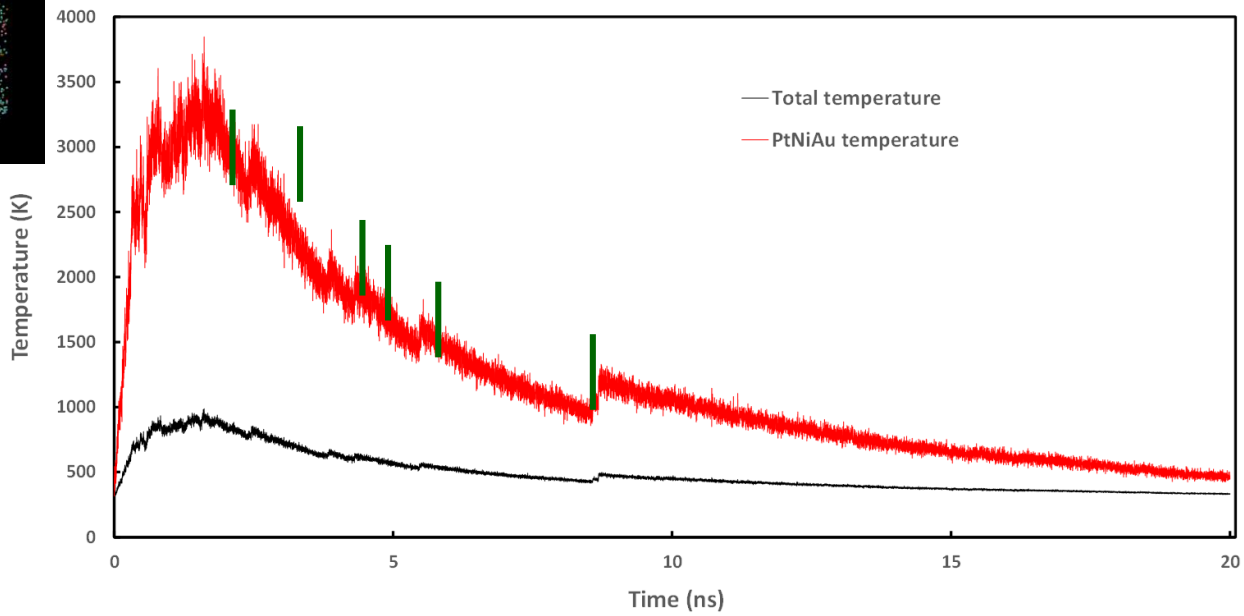

Molecular dynamics simulation of sputtering plasma catalysts growth: Free Pt_3NiAu nanocatalyst growth

Cluster 1 (318 at.) : cuboctahedron ?

$Pt_{189}Ni_{62}Au_{67} \approx Pt_3NiAu$

• Pt; • Ni; • Au

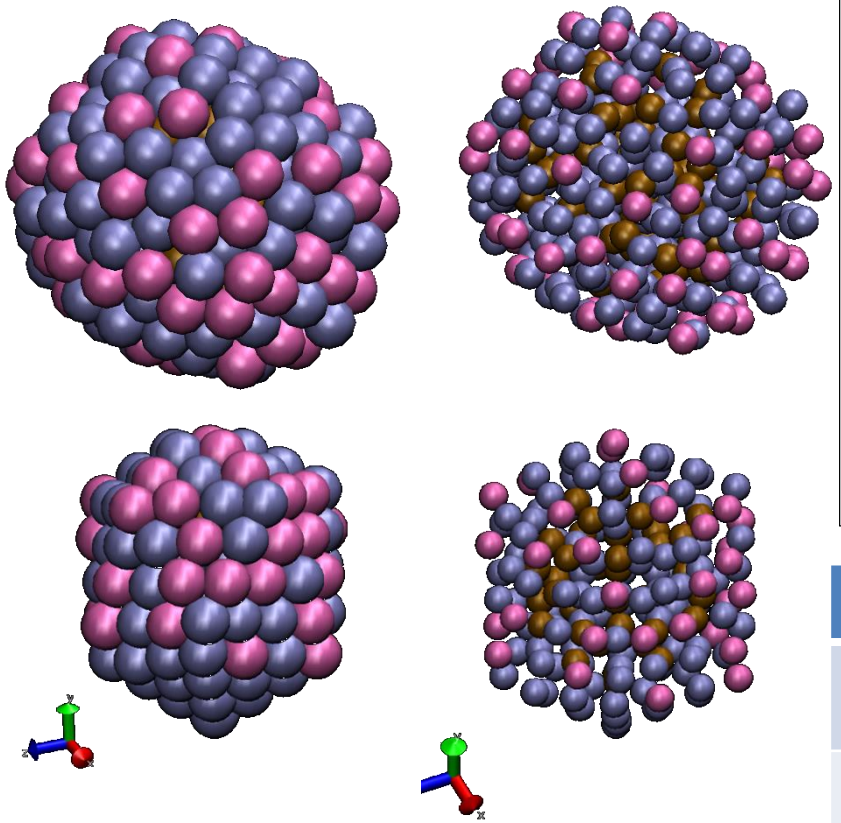

Cluster 2 (182 at.) : icosahedron ?

$Pt_{111}Ni_{38}Au_{33}$

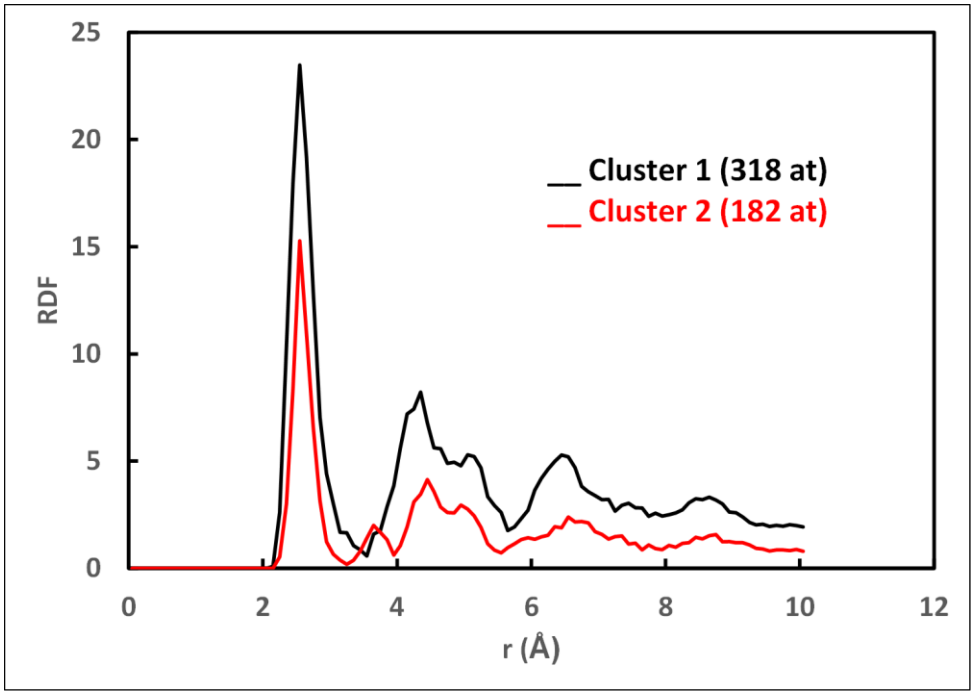

	1st NN	2nd NN	3rd NN
Theoretical (fcc) 0.6Pt+0.2Ni+0.2Au	2.738 Å	3.872 Å	4.74 Å
Cluster 1	2.55 Å	(3.75 Å)	4.35 Å
Cluster 2	2.55 Å	3.65 Å	4.45 Å

Molecular dynamics simulation of sputtering plasma catalysts growth: Pt_xB_y nanocatalyst growth

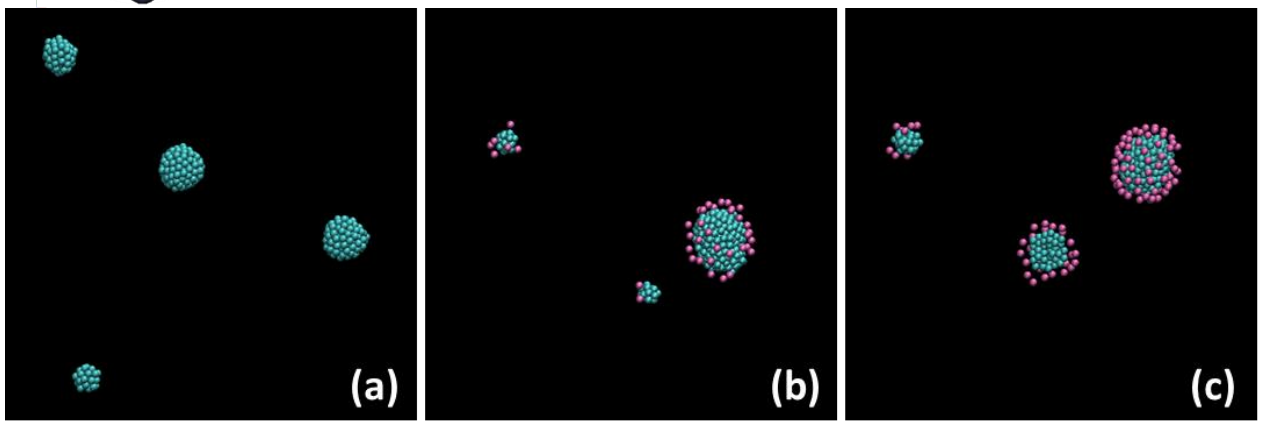

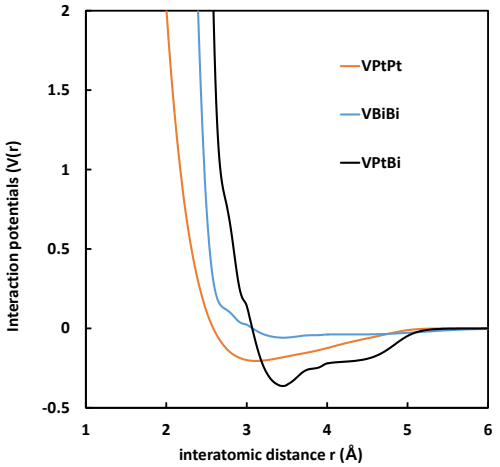

Snapshot of the final clusters at 20 ns. Argon atoms (4000) are not represented for clarity. $n_{Pt} + n_{Bi} = 500$. (a) Pt alone (b) Pt_9Bi_1 (c) Pt_8Bi_2. Box size 16x16x16 nm^3

Plots of the pair part of the EAM interaction potentials: $V_{PtPt}(r)$, $V_{BiBi}(r)$, $V_{PtBi}(r)$.

- Cluster atomic arrangements are typical of a crystalline structure of the Pt cores, with numbers of 1st nearest neighbors between 10 and 12 (i.e. consistent with fcc arrangement)
- Bi composition < 20% leads to cluster surfaces with both Pt and Bi, allowing catalytic activity enhancement.
- Pt/Bi atomic composition is not only globally preserved, but is also verified for each cluster

Molecular dynamics simulation of sputtering plasma catalysts growth: Reactive PdO nanocatalyst growth

ReaxFF reactive variable charge potentials for Pd sputtering in Ar-O_2 gas mixture

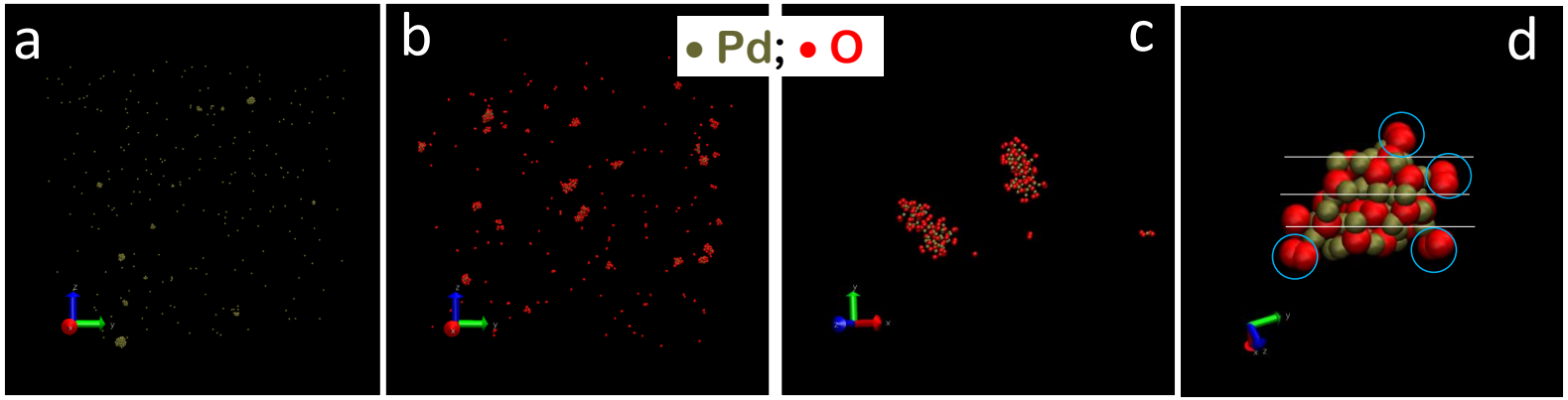

Snapshot of (a-b) the overall Pd and PdO clusters at 25 ns simulation time (b-c) of the detailed PdO clusters.

First results: O addition -> no more free Pd, more PdO than Pd clusters

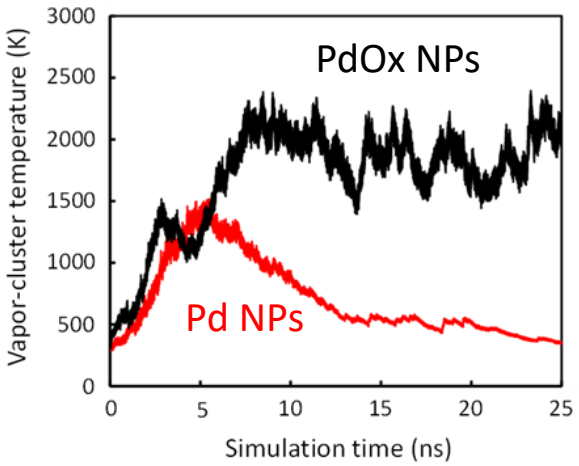

Ratio of N_{Ar} to N_{metal} estimated from experiments = 40 here;

N_{Ar} = 20000; N_{Pd} = 500; N_O = 1000; Box size : 40 x 40 x 40 nm^3

Integration time 0.25 fs → 1. 10^8 iterations

Potential ReaxFF : T. Senftle et al, J. Chem Phys 139 (2013) 044109

P. Brault et al, Molecular Dynamics simulations of initial Pd and PdO nanocluster growths in a magnetron gas aggregation source, Frontiers in Chemical Science and Engineering (2018) accepted.

Conclusions

- Magnetron sputtering deposition techniques are very powerful for designing nanocatalysts.
- GAS is a very promising variant for depositing preformed well defined nanocatalysts. Deposition rate can be high.
- (Reactive) molecular dynamics simulations are very attractive for describing/predicting sputter deposited/ grown NPs.

Perspectives
Towards full MD description of plasma processing: Principles

New reactive and including electron interaction potential allow targeting multiscale MD simulations of operating plasma reactor

1/ recovering/scaling experimental conditions

Hypothesis : Collision number are the same in experiments and simulations so, $P_{exp}d_{exp} = P_{sim}d_{sim}$ thus $N_{sim} = \frac{P_{exp}}{k_B T_g} \cdot S_{sim} \cdot d_{exp}$ and if rcut is the largest cutoff radius : $d_{sim} > \frac{N_{sim}}{S_{sim}} \cdot {r_{cut}}^3$

(S_{sim} is the chosen smallest area of the simulation box)

2/ combine improved force fields

Plasma factor	Possible?	Example
electric field	yes	CNT growth
atoms and hyperthermal species	yes	Si-NW oxidation
radicals	yes	a-C:H growth
ions	yes	sputtering
electronically excited states	yes	etching
vibrationally excited states	yes / no (reaxFF)	/
photons	implicit	(polymer degradation)
electrons	Yes (eFF, e-reaxFF)	/

E. Neyts, P. Brault (Review article), *Molecular dynamics simulations for plasma surface interactions*, Plasma Processes and Polymers 14 (2017) 1600145

Perspectives: Towards full MD description of plasma processing. Application to nanocluster growth in plasma sputtering

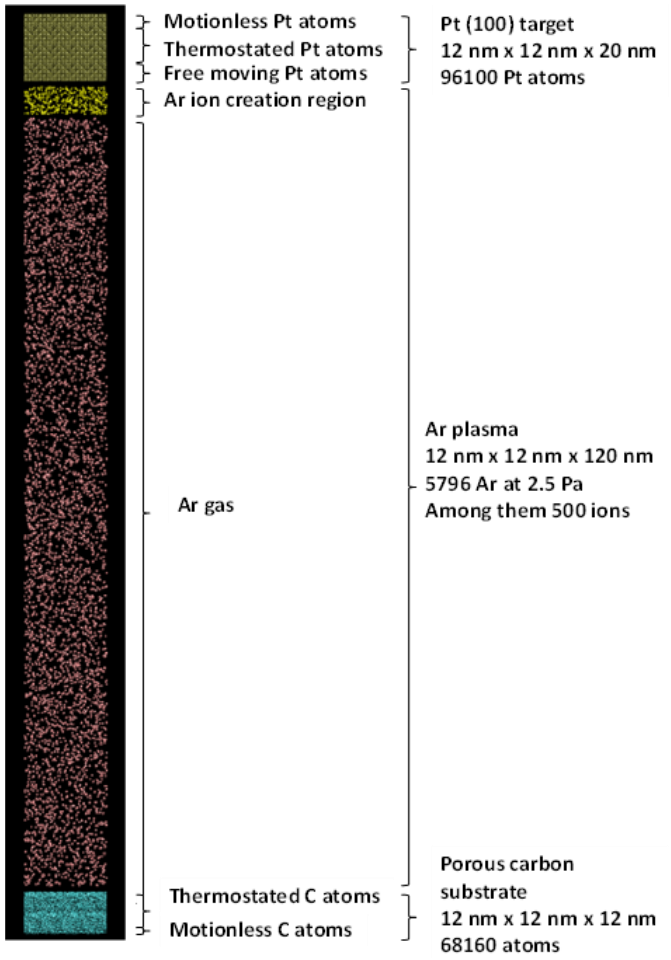

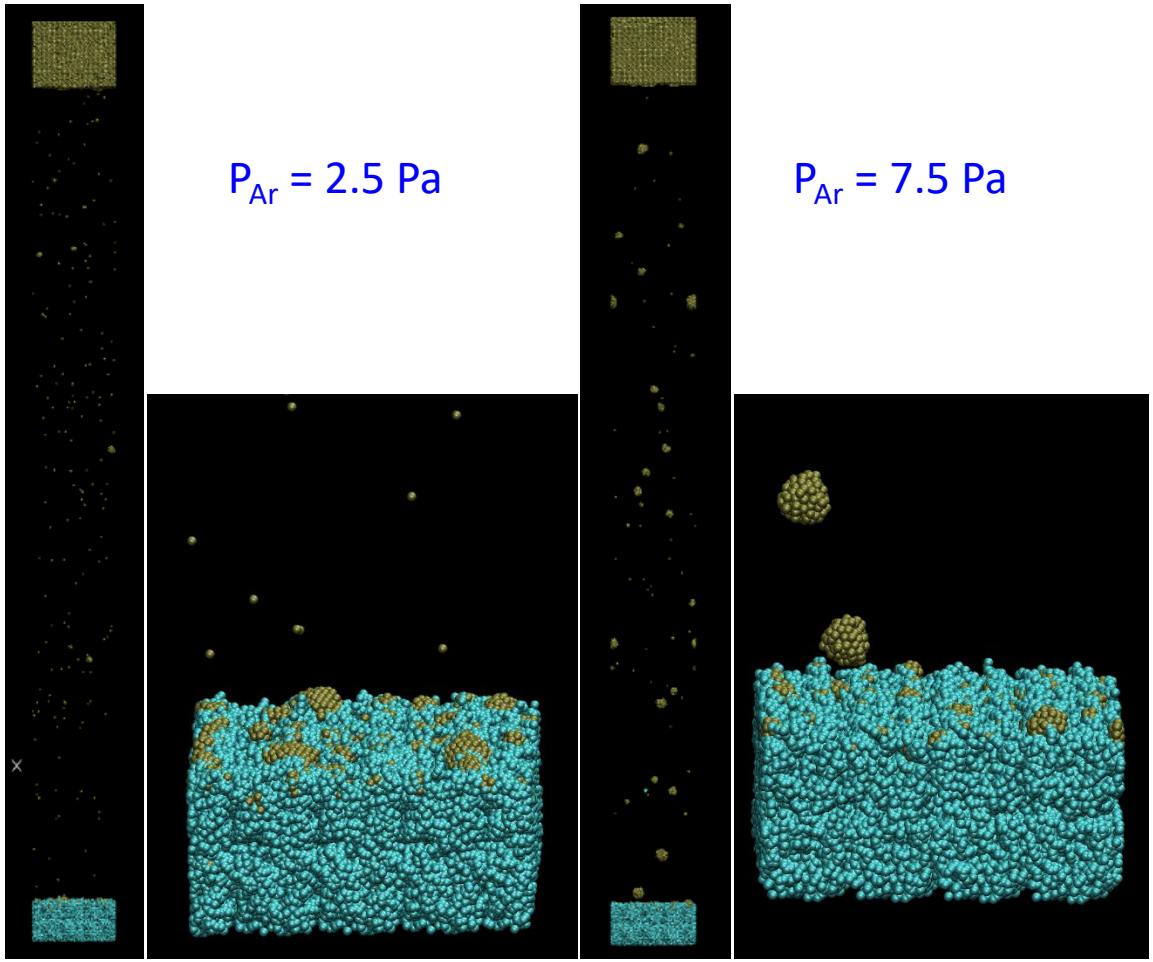

P. Brault, *Multiscale Molecular Dynamics Simulation of Plasma Processing: Application to Plasma Sputtering*, Front. Phys. 6 (2018) 59

Acknowledgements

Many thanks for your attention

Many thanks to the GREMIs' people who contribute to the work

Staff members	PhD Candidates	Postdoc	Collaborations
Anne-Lise Thomman	Aboubakr Ennadjaoui (†)	Hervé Rabat	C. Charles
Amaël Caillard	Sujuan Wu	Marjorie Cavarroc	R. Boswell
Yves Tessier	Mathieu Mougenot	William Chamorro-Coral	C. Corr, D. Ramdutt
Thomas Lecas	Lu Xie	Vanessa Orozco-Montes	D. B. Graves
Johannes Berndt	Stéphane Cuynet		E. Neyts
	Sotheara Chuon		P. & C. Andreazza